

Triple-shock entropy theorem and its consequences

By LE ROY F. HENDERSON^{1,2,3†} AND RALPH MENIKOFF⁴

¹Laboratoire d'Aerothermique du CNRS, 4ter route des Gardes, 92190 Meudon, France

²Shock Wave Research Center, Institute of Fluid Science, Tohoku University, 2-1-1 Katahira, Aoba, Sendai 980, Japan

³Department of Mechanical Engineering, Ben-Gurion University of the Negev, P.O.B. 653 Beer-Sheva 84105, Israel

⁴Theoretical Division, Los Alamos National Laboratory, Los Alamos, NM 87545, USA

(Received 23 July 1997 and in revised form 10 February 1998)

For a convex equation of state, a general theorem on shock waves is proved: a sequence of two shocks has a lower entropy than a single shock to the same final pressure. We call this the *triple-shock entropy theorem*. This theorem has important consequences for shock interactions. In one dimension the interaction of two shock waves of the opposite family always results in two outgoing shock waves. In two dimensions the intersection of three shocks, such as a Mach configuration, must have a contact. Moreover, the state behind the Mach stem has a higher entropy than the state behind the reflected shock. For the transition between a regular and Mach reflection, this suggests that the von Neumann (mechanical equilibrium) criterion would be preferred based on thermodynamic stability, i.e. maximum entropy subject to the system constraint that the total specific enthalpy is fixed. However, to explain the observed hysteresis of the transition we propose an analogy with phase transitions in which locally stable wave patterns (regular or Mach reflection) play the role of meta-stable thermodynamic states. The hysteresis effect would occur only when the transition threshold exceeds the background fluctuations. The transition threshold is affected by flow gradients in the neighbourhood of the shock intersection point and the background fluctuations are due to acoustic noise. Consequently, the occurrence of hysteresis is sensitive to the experimental design, and only under special circumstances is hysteresis observed.

1. Introduction

It is well known that the entropy change across a weak shock is third order in shock strength, as measured, for example, by the pressure difference across the shock. As a consequence, a sequence of two weak shocks has a lower entropy than a single shock to the same final pressure. Moreover, if a fixed pressure jump is obtained with multiple shocks then the entropy change vanishes in the limit of a large number of weak shocks. For an ideal gas equation of state, there are simple analytic expressions for the Hugoniot locus. These expressions can be used to show that a sequence of arbitrary strength shocks has a lower entropy than a single shock to the same final pressure. This property of shock wave entropy is generally assumed for an arbitrary

† Present address: 8 Damour Av., East Lindfield, Sydney, N.S.W. 2070, Australia.

equation of state. Here we prove that the shock entropy does indeed obey this property for a large class of materials.

We consider materials with a convex equation of state and satisfying either the weak condition, the modified medium condition or the two-dimensional stability condition. These constraints are reviewed in the next section. For now we simply note that constraints are needed to ensure all shock waves satisfy important properties that typically are assumed. Convexity of the equation of state and the weak condition imply that an entropy-increasing shock is compressive and stable in one-dimension. With the addition of the modified medium condition, one-dimensional shock interactions have a unique outcome. A further condition is required for shock waves to be stable in two-dimensions. Except in the vicinity of a phase transition, real materials satisfy these conditions: more precisely, nearly all materials in a single phase satisfy the convexity condition (Bethe 1942), while all materials known to us satisfy the modified medium condition. Moreover, planar shock fronts are stable and the equilibrium equation of state of real materials satisfies the two-dimensional stability condition. Exceptions to shock stability only occur when certain non-equilibrium processes, such as dissociation or ionization, dominate the shock profile.

For the class of materials with a convex equation of state and satisfying the weak condition we prove in §2 that the entropy behind a sequence of N shocks is lower than the entropy behind a single shock to the same final pressure. The key result is for two shocks. We call this the *triple-shock entropy theorem*. With the additional assumption of the modified medium condition, we derive a bound on the particle velocity along the Hugoniot locus for a sequence of two shocks compared to a single shock to the same final pressure. The triple-shock entropy theorem and the related velocity bound have important consequences for shock interactions in both one and two dimensions.

Our analysis of shock interactions in §3 assumes that the modified medium condition is satisfied. Using the bound on the particle velocity along the Hugoniot we show that the collision in one dimension of two shocks of the opposite wave family always results in two outgoing shock waves. By contrast, it is well known that the collision of two shocks of the same family can result in either a shock or rarefaction of the opposite family in addition to a stronger shock of the original family, see e.g. Courant & Friedrichs (1948, chap. III.D, §79).

It is common in two dimensions for oblique shocks to intersect and form distinctive wave patterns. The two-dimensional wave patterns are the natural analogue of shock interactions in one dimension. We discuss in detail one important wave pattern, known as a Mach configuration, which occurs when three shock waves intersect. Since streamlines either go through the incident and reflected shock or through the Mach stem, this wave pattern provides an example in which a sequence of two shocks naturally arises with the same final pressure as a single shock. The triple-shock entropy theorem implies that the entropy is higher behind the Mach stem than behind the reflected shock. As a consequence, a contact must occur whenever three shocks intersect. Moreover, we show that the difference in entropy along steady-state streamlines implies that shock interactions must generate vorticity.

In contrast to one dimension, questions of non-uniqueness arise for two-dimensional shock interactions. In particular, a Mach configuration represents a splitting of an incoming shock into two outgoing shocks (Landau & Lifshitz 1959, chap. X, §102). Stability of shock waves in two-dimensions requires an additional constraint on the equation of state. The two-dimensional stability condition derived from a linear stability analysis (Kontorovich 1959; Fowles 1981) also implies the weak and

medium conditions. Hence, two-dimensional stability implies that one-dimensional shock interactions are well behaved (Menikoff & Plohr 1989). We show in §4.1 that the two-dimensional stability condition can be given a physical interpretation related to a threshold for a Mach configuration to occur. Furthermore, we argue for the regular reflection to Mach reflection transition that stability favours the von Neumann (mechanical equilibrium) transition criterion. This is based on the observation that at fixed pressure the entropy of a regular reflection can be increased by creating a velocity shear layer which allows kinetic energy to be exchanged for enthalpy, i.e. transition to Mach reflection.

Finally, in §4.2 we discuss the hysteresis associated with the transition between regular and Mach reflection. A hysteresis effect was first observed by Henderson & Lozzi (1979) on curved surfaces and predicted by Hornung, Oertel & Sandeman (1979) for plane surfaces but not observed in the initial experiments of Hornung & Robinson (1982). Recent experiments and numerical simulations by Chpoun *et al.* (1995), Ivanov, Gimelshein & Beylich (1995*a,b*) Ivanov *et al.* (1995*b*), Fomin *et al.* (1996), Skews (1996) show that in some circumstances the transition does exhibit a hysteresis effect. The hysteresis effect implies that both regular and Mach reflection are locally stable and hence a simple transition criterion is inadequate.

To explain the experimental result that hysteresis is only observed under limited circumstances, we utilize an analogy with phase transitions. This leads to the hypothesis that the bifurcation or transition between locally stable wave patterns can be triggered only by a perturbation above a threshold amplitude. Since both the noise level and the threshold amplitude depend on the experimental design, it is not surprising that hysteresis behaviour is observed in some experiments but not in others. In particular, transverse gradients from three-dimensional disturbances can have a significant effect on the transition (Ivanov *et al.* 1995; Fomin *et al.* 1996; Skews 1996).

2. Properties of the shock Hugoniot

In this section, properties of the Hugoniot locus are derived for a large class of materials. We assume a material is in local thermodynamic equilibrium and can be characterized by an equilibrium *equation of state* (EOS). We require the EOS to satisfy the following physical properties.

(1) Thermodynamic phase space is parameterized by (V, S) where $V = 1/\rho$ is the specific volume, ρ is the density and S is the entropy. A complete EOS is specified by the specific internal energy $e(V, S)$.

(2) Thermodynamic consistency requires that the fundamental thermodynamic identity is satisfied:

$$de = -PdV + TdS, \quad (2.1)$$

where P is the pressure and T is the temperature.

(3) The temperature is always positive. Since a temperature of absolute zero can not be physically obtained, we may assume that $T > 0$.

(4) Every isentrope satisfies the asymptotic conditions that (i) $P \rightarrow \infty$ as $V \rightarrow 0$, and (ii) $P \rightarrow 0$ as $V \rightarrow \infty$.

(5) For any V , the pressure becomes arbitrarily large as S increases, i.e. $P(V, S) \rightarrow \infty$ as $S \rightarrow \infty$ for fixed V .

In addition, we assume that the equation of state is convex, i.e. in the (V, P) -plane every isentrope is convex. Except in the vicinity of phase transitions, isentropes of real materials are convex.

From the conservation laws for mass, momentum and energy, a shock wave satisfies the Hugoniot equation

$$e_1 - e_0 = \frac{1}{2}(P_0 + P_1)(V_0 - V_1), \quad (2.2)$$

where the subscripts 0 and 1 denote the states ahead of and behind the shock, respectively. The shock speed, σ , is determined by the relation

$$[\rho_0(\sigma - u_0)]^2 = [\rho_1(\sigma - u_1)]^2 = (P_1 - P_0)/(V_0 - V_1), \quad (2.3)$$

and the change in the particle velocity, u , is given by

$$(u_1 - u_0)^2 = (P_1 - P_0)(V_0 - V_1). \quad (2.4)$$

For the wave speed and particle velocity, the sign of the square root determines the wave family i.e., right facing (characteristic $u+c$) or left facing (characteristic $u-c$). We assume the initial state (V_0, e_0, u_0) is specified, and refer to the Hugoniot locus based on the state 0 as the set of all states that can be reached from state 0 by a shock wave. The shock state and wave speed for a given wave family are completely determined by (2.2), (2.3) and (2.4), and the EOS, i.e. $P_0 = P(V_0, e_0)$ and $P_1 = P(V_1, e_1)$. Though the Hugoniot locus depends explicitly only on an incomplete EOS, $P = P(V, e)$, its properties depend on the existence of a complete EOS.

We will use three dimensionless parameters to characterize an equation of state.

The *adiabatic exponent*

$$\gamma \equiv -\frac{V}{P} \left. \frac{\partial P}{\partial V} \right|_S = \frac{c^2}{PV} \quad (2.5)$$

is a dimensionless form for the sound speed c . Thermodynamic stability requires $\gamma \geq 0$.

The *Grüneisen coefficient*

$$\Gamma \equiv V \left. \frac{\partial P}{\partial e} \right|_V = \frac{V}{T} \left. \frac{\partial P}{\partial S} \right|_V \quad (2.6)$$

measures the spacing of the isentropes in the (V, P) -plane.

Using these parameters, the fundamental thermodynamic relation can be expressed as

$$VdP = -\gamma PdV + \Gamma T dS. \quad (2.7)$$

The *fundamental derivative*

$$\mathcal{G} \equiv -\frac{1}{2}V \frac{\partial^2 P / \partial V^2|_S}{\partial P / \partial V|_S} \quad (2.8)$$

is a measure of the convexity of an isentrope in the (V, P) -plane. For a convex EOS $\mathcal{G} > 0$ everywhere. Moreover, $\mathcal{G} > 0$ excludes $\gamma = 0$ and hence implies that $\gamma > 0$ everywhere.

In order for fluid flow (solution to the compressible Euler equations) to be well behaved, one-dimensional Riemann problems must have a unique solution. This requires that both the pressure and particle velocity are monotonic along the Hugoniot locus. Three constraints on an EOS have been proposed to ensure monotonicity of the state variables along the Hugoniot locus; they are called the strong, medium and weak condition, see Menikoff & Plohr (1989 and references contained therein). In addition, there is a slightly stronger variation or modified medium condition which is equivalent to the ‘shock splitting’ condition (III) of Bethe (1942). The weak condition,

$\Gamma \leq 2\gamma$, is sufficient for the pressure to be monotonic and the modified medium condition, $\Gamma \leq \gamma$, is sufficient for both pressure and particle velocity to be monotonic. A stronger stability condition, $\Gamma \leq \gamma - 1$, is needed in order for strong shock waves to be stable to small perturbations in multi-dimensions.

The triple-shock entropy theorem requires $\mathcal{G} > 0$ and the weak condition. The analysis of the particle velocity along the Hugoniot locus requires in addition the modified medium condition. Both the weak and modified medium condition follow from the two-dimensional stability condition. Thus, our assumptions are physically reasonable and are only mild constraints on an equation of state. We do not assume $\Gamma > 0$ everywhere. Consequently, the (V, P) -plane does not uniquely parameterize phase space. Since $\gamma > 0$, a given isentrope can be parameterized by either V or P . Consequently, thermodynamic phase space can be uniquely parameterized by either the (V, S) -plane or the (P, S) -plane.

2.1. Preliminary results

The Hugoniot locus based on the state 0 corresponds to the zero-level set of the Hugoniot function. In the (V, S) -plane, the Hugoniot function is given by

$$h(V, S) = e(V, S) - e_0 - \frac{1}{2} [P(V, S) + P_0] (V_0 - V). \quad (2.9)$$

The equivalent function in the (P, S) -plane is

$$\begin{aligned} \tilde{h}(P, S) &= h(V(P, S), S) \\ &= H(P, S) - H_0 - \frac{1}{2} [V(P, S) + V_0] (P - P_0), \end{aligned} \quad (2.10)$$

where $H = e + PV$ is the specific enthalpy.

Our analysis utilizes the differential of the Hugoniot function. Taking the differential of (2.9) and (2.10) and substituting the thermodynamic relations (2.1) and (2.7) we obtain

$$dh = \left(1 + \frac{1}{2}\Gamma \frac{\Delta V}{V}\right) T dS - \frac{1}{2} \left(\gamma \frac{\Delta V}{V} + \frac{\Delta P}{P}\right) P dV, \quad (2.11)$$

$$d\tilde{h} = \left(1 - \frac{\Gamma}{2\gamma} \frac{\Delta P}{P}\right) T dS + \frac{1}{2\gamma} \left(\gamma \frac{\Delta V}{V} + \frac{\Delta P}{P}\right) V dP, \quad (2.12)$$

where $\Delta f = f - f_0$ is the difference of the variable f with respect to its value at the initial state. From (2.12) we obtain

$$\left. \frac{\partial \tilde{h}}{\partial S} \right|_P = \left(1 - \frac{\Gamma}{2\gamma} \frac{\Delta P}{P}\right) T. \quad (2.13)$$

We note that $0 \leq \Delta P/P < 1$ if $P \geq P_0$ and $\Gamma/2\gamma \leq 1$ if the weak condition holds. The importance of the weak condition stems from the fact that

$$\left. \frac{\partial \tilde{h}}{\partial S} \right|_P > 0, \quad \text{if } P \geq P_0 \quad \text{and} \quad \Gamma \leq 2\gamma. \quad (2.14)$$

The Hugoniot function reduces the problem of determining the Hugoniot locus to finding the solution of a single equation in two variables: either V and S , or P and S . In order for σ and u_1 to be real, and hence to have a solution to the three Rankine–Hugoniot jump conditions, it is necessary that $\Delta P \Delta V \leq 0$.

LEMMA 1. *The Hugoniot function associated with the state 0 has no zeros when $\Delta P \cdot \Delta V \geq 0$ except for the point $(V, P) = (V_0, P_0)$.*

Proof. Let (V, P) be any point in the quadrant $\Delta P \geq 0, \Delta V \geq 0$ with $(V, P) \neq (V_0, P_0)$. If $S < S_0$ then the Hugoniot function can be expressed as

$$h(V, S) = h(V_0, S_0) + \int_{S_0}^S \partial_S h \, dS \Big|_{V_0} + \int_{V_0}^V \partial_V h \, dV \Big|_S.$$

We note that (i) $h(V_0, S_0) = 0$, (ii) $\partial_S h|_{V_0} = T > 0$, and (iii) $\partial_V h|_S = -\frac{1}{2}(\gamma \Delta V/V + \Delta P/P)P < 0$. Consequently, $h(V, S) < 0$.

Similarly, if $S > S_0$ then

$$\tilde{h}(P, S) = \tilde{h}(P_0, S_0) + \int_{S_0}^S \partial_S \tilde{h} \, dS \Big|_{P_0} + \int_{P_0}^P \partial_P \tilde{h} \, dP \Big|_S.$$

We note that (i) $\tilde{h}(P_0, S_0) = 0$, (ii) $\partial_S \tilde{h}|_{P_0} = T > 0$, and (iii) $\partial_P \tilde{h}|_S = (2\gamma)^{-1}(\gamma \Delta V/V + \Delta P/P)V > 0$. Consequently, $\tilde{h}(P, S) > 0$. Hence, the Hugoniot function is not zero in the quadrant $\Delta P \geq 0, \Delta V \geq 0$ provided that the point (V_0, P_0) is excluded.

The Hugoniot equation is invariant when the initial and final states are interchanged. Interchanging the initial and final shock states interchanges the two quadrants $\Delta P \geq 0, \Delta V \geq 0$ and $\Delta P \leq 0, \Delta V \leq 0$. Hence the Hugoniot function is not zero when $\Delta P \Delta V \geq 0$ except for the point (V_0, P_0) . \square

This Lemma implies that there are no extraneous solutions to the Hugoniot equation, i.e. there is a one-to-one correspondence between solutions to the Hugoniot equation and points on Hugoniot locus for each wave family.

The Bethe–Weyl theorem is important for a convex EOS. It implies that the Hugoniot locus can be parameterized by the entropy and consists of a single curve connected to the initial state. We correct an error in the proof given in Menikoff & Plohr (1989).[†] It is useful to consider points on the Hugoniot locus based on the state 0 with a given entropy S . These points correspond to the zero-level set of the restricted Hugoniot function

$$h_S(V) = e(V, S) - e_0 - \frac{1}{2} [P(V, S) + P_0] (V_0 - V), \quad (2.15)$$

or equivalently

$$\tilde{h}_S(P) = H(P, S) - H_0 - \frac{1}{2} [V(P, S) + V_0] (P - P_0).$$

Taking the first two derivatives of (2.15) we obtain

$$h'_S(V) = -\frac{1}{2} \left(P(V, S) - P_0 - \frac{\partial P}{\partial V} \Big|_S (V - V_0) \right), \quad (2.16)$$

$$h''_S(V) = \frac{1}{2} (V - V_0) \frac{\partial^2 P}{\partial V^2} \Big|_S. \quad (2.17)$$

The initial isentrope is an important reference curve. We note that

$$h_{S_0}(V_0) = h'_{S_0}(V_0) = h''_{S_0}(V_0) = 0.$$

[†] In (4.13) of Menikoff & Plohr (1989), P_0 which is equal to $P(V_0, S_0)$ was inadvertently substituted for $P(V_0, S)$. As a consequence, an additional condition is needed to rule out a disconnected branch of the Hugoniot locus with entropy-increasing expansive shocks or entropy-decreasing compressive shocks. Either Bethe's condition $\Gamma \geq -2$ or the weak condition $\Gamma \leq 2\gamma$ are sufficient to recover theorem 4.1 of Menikoff & Plohr (1989).

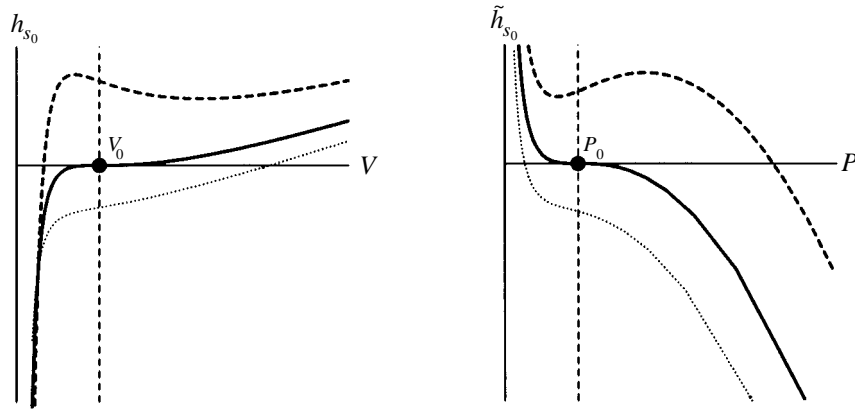


FIGURE 1. The essential geometry of the restricted Hugoniot function. The dotted, solid and dashed lines correspond to $S < S_0$, $S = S_0$ and $S > S_0$, respectively.

Moreover, for a convex EOS $(\partial^2 P / \partial V^2)|_S > 0$, and by (2.17)

$$h''_{s_0}(V) \begin{cases} < 0 & \text{for } V < V_0 \\ > 0 & \text{for } V > V_0. \end{cases}$$

Therefore, $h_{s_0}(V)$ has an inflection point at $V = V_0$ and is monotonically increasing over the entire range $0 < V < \infty$. In particular,

$$h_{s_0}(V) < 0 \quad \text{for } V < V_0. \tag{2.18}$$

Since $\tilde{h}_{s_0}(P) = h_{s_0}(V(P, S_0))$ and $(\partial P / \partial V)|_S < 0$, it follows that

$$\tilde{h}_{s_0}(P) < 0 \quad \text{for } P > P_0. \tag{2.19}$$

As an illustrative example, for an ideal gas EOS the restricted Hugoniot function along the initial isentrope is shown in figure 1 by the solid line.

We now exclude anomalous shocks.

LEMMA 2. *If $\mathcal{G} > 0$ and $\Gamma \leq 2\gamma$ then there are no entropy-increasing expansive shocks and no entropy-decreasing compressive shocks.*

Proof. The Hugoniot function can be expressed as

$$\tilde{h}(P, S) = \tilde{h}_{s_0}(P) + \int_{S_0}^S \left. \frac{\partial \tilde{h}}{\partial S} \right|_P dS.$$

From (2.19), the first term on the right-hand side is negative for $P > P_0$. From (2.14) the integrand is positive. Hence the integral is negative for $S < S_0$. Therefore, $\tilde{h}(P, S) < 0$ for entropy-decreasing compressive shocks. Since interchanging the initial and final states converts an entropy-decreasing compressive shock into an entropy-increasing expansive shock, both of these anomalous shocks are excluded. \square

We note that for a non-convex EOS entropy-increasing expansive shocks are required for the existence of solutions to Riemann problems since a rarefaction curve ends when $\mathcal{G} = 0$, see e.g. Zel'dovich & Raizer (1967, chap. XI, § 20). Thus, anomalous shocks are allowed by thermodynamics but are excluded by our assumption that the equation of state is convex.

Next we show that the weak condition implies that compressive shocks can be parameterized by P and that the Hugoniot locus extends up to $P = \infty$.

LEMMA 3. *If $\mathcal{G} > 0$ and $\Gamma \leq 2\gamma$ then the Hugoniot locus based on state 0 contains a unique shock for any $P \geq P_0$. Moreover, pressure-increasing shocks are entropy increasing.*

Proof. By (2.14), for any fixed $P \geq P_0$, $\tilde{h}(P, S)$ is a monotonic function of S , and therefore has at most one zero. Moreover, by (2.19), $\tilde{h}(P, S_0) < 0$ for $P > P_0$. If we can find an S' such that $\tilde{h}(P, S') > 0$ then by continuity $\tilde{h}(P, S)$ would have a unique zero for any $P > P_0$. From EOS property (5) and continuity, there exists an $S' > S_0$ such that $P = P(V_0, S')$. Since $h(V_0, S_0) = 0$ and from (2.11), $(\partial h / \partial S)|_V(V_0, S) = T > 0$, it follows that $\tilde{h}(P, S') = h(V_0, S') > 0$. Hence, we can conclude that $\tilde{h}(P, S)$ has a unique zero for any $P > P_0$. Therefore, there is a unique shock for any $P > P_0$, and it is entropy increasing. \square

For a convex EOS satisfying the weak condition we can obtain the first key result.

THEOREM 1 (BETHE–WEYL). *If $\mathcal{G} > 0$ and $\Gamma \leq 2\gamma$ then the Hugoniot locus based on any state 0 intersects every isentrope exactly once. Moreover, for entropy-increasing shocks $V < V_0$ and $|u - \sigma| < c$, while for entropy-decreasing shocks $V > V_0$ and $|u - \sigma| > c$.*

Proof. From the asymptotic EOS conditions, it follows that $h_S(V) \rightarrow -\infty$ as $V \rightarrow 0$ and $h_S(V) \rightarrow \infty$ as $V \rightarrow \infty$; see Menikoff & Plohr (1989). By continuity, there is at least one shock state for every S . By Lemmas 1 and 2 shocks are either compressive and entropy increasing or expansive and entropy decreasing. First, we consider the entropy-increasing case: $S > S_0$ and $V < V_0$. From (2.15) and (2.1)

$$h_S(V_0) = e(V_0, S) - e_0 = \int_{S_0}^S T dS \Big|_{V_0} > 0.$$

Moreover, $h_S(V) \rightarrow -\infty$ as $V \rightarrow 0$ and from (2.17) $h'_S(V) < 0$. Hence, $h_S(V)$ is concave in the domain $0 < V < V_0$. Therefore, $h_S(V)$ has a unique zero. Furthermore, at the zero crossing $h'_S > 0$. The dashed line in figure 1 illustrates the restricted Hugoniot function for this case.

At the zero crossing, using (2.3) and (2.5), we can rewrite (2.16) as

$$\begin{aligned} 0 < 2 \frac{h'_S(V)}{V_0 - V} &= \frac{\Delta P}{\Delta V} - \frac{\partial P}{\partial V} \Big|_S \\ &= \rho^2 [-(\sigma - u)^2 + c^2]. \end{aligned}$$

Therefore, $|\sigma - u| < c$. A similar argument can be applied to obtain the analogous result in the entropy decreasing case. \square

A continuity argument allows us to characterize the Hugoniot locus as follows.

COROLLARY 1. *If $\mathcal{G} > 0$ and $\Gamma \leq 2\gamma$ then the Hugoniot locus can be parameterized by S and consists of a single curve connected to the base state.*

Proof. From the Bethe–Weyl theorem, the base state 0 is the only sonic state on

the Hugoniot locus. By (2.12), along the Hugoniot locus

$$\left. \frac{\partial \tilde{h}}{\partial P} \right|_S = \frac{1}{2\gamma} \left(\gamma \frac{\Delta V}{V} + \frac{\Delta P}{P} \right) V \neq 0$$

for $S \neq S_0$. Since the Hugoniot locus corresponds to $\tilde{h}(P, S) = 0$, the implicit value theorem (see Appendix A) implies that the Hugoniot locus can locally be parameterized by S except at S_0 . From the Bethe–Weyl theorem, there is a unique shock for each S . Therefore, the local patches can be pieced together to give a connected entropy-increasing branch and a connected entropy-decreasing branch. In the vicinity of S_0 , an additional argument is needed because of the well known fact that for weak shocks the entropy change is third order. We note that $(\partial \tilde{h} / \partial S)|_P(P_0, S_0) = T_0 > 0$. The implicit value theorem implies that weak shocks can locally be parameterized by P . Because there is unique shock for each S , the Hugoniot locus can be parameterized by S in a local neighbourhood of S_0 . This connects the entropy-increasing and entropy-decreasing branch. Therefore, the Hugoniot locus consists of a single branch. It can be parameterized by S and is connected to the initial state. \square

The following is an important consequence of the Bethe–Weyl theorem that we will need for the triple-shock entropy theorem.

COROLLARY 2. *If $\mathcal{G} > 0$ and $\Gamma \leq 2\gamma$ then for an entropy-increasing shock the ahead state is supersonic and the behind state is subsonic.*

Proof. From the Bethe–Weyl theorem an entropy-increasing shock is compressive. The behind state is subsonic since $c > |\sigma - u|$. Interchanging the initial and final state results in an entropy-decreasing expansive shock. The equations for the wave speed and particle velocity, (2.3) and (2.4), are symmetric in the shock states. Hence, it follows from the Bethe–Weyl theorem that $c_0 < |\sigma - u_0|$ and the ahead state is supersonic. \square

2.2. Main theorem

We can now prove our main result.

THEOREM 2 (TRIPLE-SHOCK ENTROPY THEOREM). *Suppose $\mathcal{G} > 0$ and $\Gamma \leq 2\gamma$ are satisfied everywhere. Consider only the physical entropy-increasing shocks. Then a sequence of two shocks has a smaller entropy than a single shock to the same final pressure.*

Proof. Suppose the material is initially in state 0. Let state 1 be a point on the shock Hugoniot based on state 0, and let state 2 be a point on the shock Hugoniot based on state 1. By Lemma 3 there is a unique state 2' on the Hugoniot locus based on state 0 such that $P_{2'} = P_2$. With this notation, the theorem can be stated as $S_2 < S_{2'}$.

We specify a shock by its end states, e.g. shock 0-1 denotes the shock connecting state 0 to state 1. From the Hugoniot equations for shocks 1-2 and 0-1

$$\begin{aligned} e_2 - e_1 &= \frac{1}{2} (P_1 + P_2) (V_1 - V_2), \\ e_1 - e_0 &= \frac{1}{2} (P_0 + P_1) (V_0 - V_1). \end{aligned}$$

Adding these equation we obtain

$$e_2 - e_0 = \frac{1}{2} (P_1 + P_2) (V_1 - V_2) + \frac{1}{2} (P_0 + P_1) (V_0 - V_1). \quad (2.20)$$

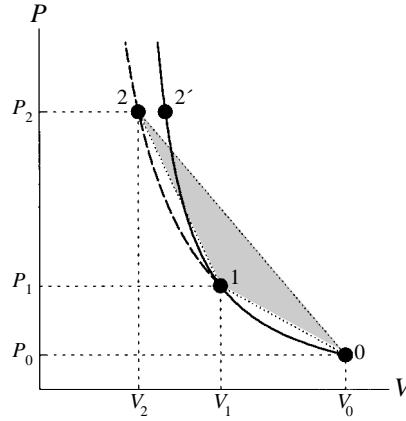


FIGURE 2. Geometry of Hugoniot loci in the (V, P) -plane used in proof of triple-shock theorem. The solid line and dashed lines are Hugoniot loci based on states 0 and 1 respectively. The dotted lines correspond to the Rayleigh lines connecting the end states of shocks 0-1, 1-2 and 0-2'. The shaded area is the triangle formed by the states 0, 1, and 2.

The restricted Hugoniot function based on state 0 with entropy S_2 is

$$h_{S_2}(V) = e(V, S_2) - e_0 - \frac{1}{2}[P_0 + P(V, S_2)](V_0 - V).$$

Evaluating at $V = V_2$ and substituting (2.20) to eliminate $e_2 - e_0$ yields

$$h_{S_2}(V_2) = \frac{1}{2}(P_1 + P_2)(V_1 - V_2) + \frac{1}{2}(P_0 + P_1)(V_0 - V_1) - \frac{1}{2}(P_0 + P_2)(V_0 - V_2).$$

Each term on the right-hand side corresponds to the area of a trapezoid in the (V, P) -plane. By the Bethe–Weyl theorem, the entropy-increasing shocks are compressive. Hence, $V_2 < V_1 < V_0$. It then follows from the geometry (shown in figure 2) that

$$h_{S_2}(V_2) = \left[\begin{array}{l} \text{signed area of triangle connecting} \\ \text{points } (V_0, P_0), (V_1, P_1) \text{ and } (V_2, P_2) \end{array} \right], \quad (2.21)$$

where the area is positive if the point (V_2, P_2) lies below the line connecting (V_0, P_0) , (V_1, P_1) .

By Corollary 2 the state behind shock 0-1 is subsonic and the state ahead of shock 1-2 is supersonic. From (2.3) and $c^2 = -V^2(\partial P/\partial V)|_S$, we obtain

$$\begin{aligned} [\rho_1(\sigma_{01} - u_1)]^2 &< (\rho_1 c_1)^2 < [\rho_1(\sigma_{12} - u_1)]^2 \\ \frac{P_1 - P_0}{V_0 - V_1} &< -V_1^2 \left. \frac{\partial P}{\partial V} \right|_S (V_1, S_1) < \frac{P_2 - P_1}{V_1 - V_2}. \end{aligned}$$

Therefore, in the (V, P) -plane state 2 lies above the line connecting states 0 and state 1. It then follows from (2.21) that $h_{S_2}(V_2) < 0$. Hence, $\tilde{h}(P_2, S_2) < 0$. By (2.14), $\partial \tilde{h}/\partial S|_P > 0$. Therefore, the zero of $\tilde{h}(P_2, S)$ occurs for $S_2' > S_2$. \square

COROLLARY 3. *A sequence of N shocks has less entropy than a single strong shock to the same pressure.*

Proof. The triple-shock entropy theorem is a special case of the Corollary for $N = 2$. The proof for N shocks is by induction. Suppose the corollary is true for $N - 1$ shocks, then we need to extend it to N shocks. Let the initial state be denoted

0 and the state behind the shocks be denoted $1, 2, \dots, N$. Let α denote the state behind a single shock from state 0 to a pressure P_N , and let β denote the state behind a single shock from state 1 to a pressure P_N . By the triple-shock entropy theorem $S_\beta < S_\alpha$. Applying the corollary to the $N - 1$ shocks from state 1 to state N , we have $S_N < S_\beta$. Therefore, $S_N < S_\alpha$. By induction the corollary is true for any N . \square

A thermodynamic state is uniquely determined by S and P . From thermodynamic identities, the following differential relations can be derived for other thermodynamic variables of interest, see for example, Appendix A in Menikoff & Plohr (1989):

$$dH = VdP + TdS, \quad (2.22)$$

$$\frac{PV}{T}dT = \frac{\Gamma}{\gamma}VdP + \frac{\gamma g - \Gamma^2}{\gamma}TdS, \quad (2.23)$$

$$\gamma de = VdP + (\gamma - \Gamma)TdS, \quad (2.24)$$

$$\gamma PdV = -VdP + \Gamma TdS, \quad (2.25)$$

where $g = PV/C_V T > 0$ is a dimensionless inverse specific heat. We also note that thermodynamic stability requires the entropy to be jointly concave in the variables V and e . This implies that $\gamma g \geq \Gamma^2$. These relations enable us to extend the triple-shock entropy theorem to the other thermodynamic variables.

COROLLARY 4. *Consider the state behind a sequence of shocks to the same final pressure as a single shock. The multiple shocks have a lower enthalpy and lower temperature than a single shock. Moreover, if $\Gamma \leq \gamma$ then multiple shocks have a lower specific energy, and if $\Gamma > 0$ then multiple shocks have a lower specific volume.*

Proof. By Corollary 3 multiple shocks to the same P as a single shock have a lower entropy. From (2.22) and (2.23), $(\partial H/\partial S)|_P > 0$ and $(\partial T/\partial S)|_P > 0$. Hence multiple shocks have a lower enthalpy and temperature. With the additional condition $\Gamma < \gamma$, then by (2.24) $(\partial e/\partial S)|_P > 0$ and the specific energy is lower for multiple shocks. Finally, if $\Gamma > 0$ then by (2.25) $(\partial V/\partial S)|_P > 0$ and multiple shocks have a lower specific volume or higher density. \square

With the additional assumption of the modified medium condition, we can obtain a similar result for the particle velocity (denoted by u) as for the thermodynamic variables.

THEOREM 3. *Suppose $\mathcal{G} > 0$ and $\Gamma \leq \gamma$ are satisfied everywhere. Consider a sequence of two entropy-increasing shocks from state 0 to state 1 and from state 1 to state 2, and a third shock from state 0 to state 2' with $P_{2'} = P_2$. Then*

$$(u_2 - u_1)^2 + (u_1 - u_0)^2 < (u_{2'} - u_0)^2. \quad (2.26)$$

Proof. Combining equations (2.2) and (2.4) a point on the Hugoniot locus based on state 0 satisfies

$$e - e_0 = \frac{1}{2}(u - u_0)^2 + P_0(V_0 - V).$$

For the three shock 0-1, 1-2 and 0-2' we have

$$e_1 - e_0 = \frac{1}{2}(u_1 - u_0)^2 + P_0(V_0 - V_1),$$

$$e_2 - e_1 = \frac{1}{2}(u_2 - u_1)^2 + P_1(V_1 - V_2),$$

$$e_{2'} - e_0 = \frac{1}{2}(u_{2'} - u_0)^2 + P_0(V_0 - V_{2'}).$$

Subtracting the third equation from the sum of the first two equations yields

$$\frac{1}{2} [(u_{2'} - u_0)^2 - (u_2 - u_1)^2 - (u_1 - u_0)^2] = (P_1 - P_0)(V_1 - V_2) + (e_{2'} - e_2) + P_0(V_{2'} - V_2). \quad (2.27)$$

On the right-hand side, the first term is positive since entropy-increasing shocks are pressure increasing ($P_1 > P_0$ for shock 0-1) and compressive ($V_2 < V_1$ for shock 1-2). Since $P_2 = P_{2'}$, using (2.24) and (2.25) the next two terms can be expressed as

$$(e_{2'} - e_2) + P_0(V_{2'} - V_2) = \int_{S_2}^{S_{2'}} \left(1 - \frac{\Gamma}{\gamma} \frac{P_2 - P_0}{P_2} \right) T \, dS \Big|_{P_2}. \quad (2.28)$$

The integrand is positive since $\Gamma/\gamma \leq 1$ and $0 < (P_2 - P_0)/P_2 < 1$. By the triple-shock entropy theorem, $S_2 < S_{2'}$. Hence, the right-hand side of (2.27) is positive and inequality (2.26) holds. \square

We now have bounds on all the hydrodynamic variables for the state behind a sequence of shocks in terms of the corresponding variables behind a single shock to the same final pressure. These bounds have important consequences for shock interactions.

3. Shock interactions

In a shock interaction two incoming waves give rise to several outgoing waves, one for each wave family. The possible outcomes are determined by applying the conservation laws in the local neighbourhood of the singular point at which the shock waves intersect. The question of non-uniqueness is addressed in the next section. For the fluid equations, in one-dimension there are three wave families and hence three outgoing waves. The fluid equations for steady supersonic two-dimensional flow are also hyperbolic. Oblique shocks in two dimensions satisfy the one-dimensional Hugoniot equations in the direction normal to the shock front. Even though there is one additional equation in two dimensions, the system of equations has only three wave families since the characteristic associated with the particle trajectory has a multiplicity of two, corresponding to advection of both entropy and vorticity. A shock interaction is characterized in one dimension by a wave diagram in the (x, t) -plane and in two dimensions by a steady wave pattern in the (x, y) -plane. When the stream direction is viewed as the time like direction, two-dimensional wave patterns are quite similar to one-dimensional wave diagrams. In both cases, two incoming waves give rise to three outgoing waves.

One wave family is linearly degenerate and corresponds to contacts. The other two families are non-degenerate and are associated with acoustic waves. The interaction of two shock waves determines a Riemann problem. Because one wave family is linearly degenerate the fluid equations are similar to a 2×2 system, and as described below the outgoing waves in the solution can be determined with a graphical analysis utilizing the concept of a wave curve. A wave curve is the locus of states behind a scale-invariant wave with a fixed initial state and of a given wave family. For a convex equation of state, the wave curve for each acoustic mode corresponds to pressure-increasing shock waves and pressure-decreasing rarefaction waves. Here we focus on the portion of the wave curve determined by the Hugoniot locus.

The acoustic wave families in one dimension are associated with the characteristic velocities $u - c$ and $u + c$, and the corresponding shock waves are referred to as left and right facing. The moment of impact between two incoming shock waves defines

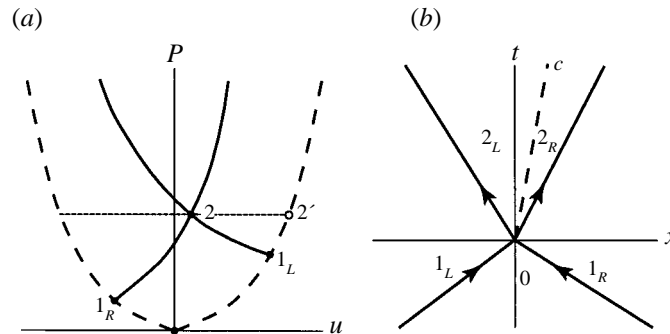


FIGURE 3. The collision of two shocks of the opposite family. (a) The projection of the Hugoniot loci in the (u, P) -plane. The dashed lines are Hugoniot loci for the incoming shocks. The solid lines are the Hugoniot loci for the outgoing shocks. The outgoing waves of the shock interaction correspond to the intersection point of the two solid curves. (b) Wave diagram in the (x, t) -plane. The initial state is labelled 0. The incoming shocks are labelled 1 and the outgoing shocks are labelled 2. The subscripts L and R denote the left and right states in the (x, t) -plane. The label 2' denotes a single shock from the initial state with the same final pressure as the outgoing waves.

the initial conditions of a Riemann problem. Across a contact the particle velocity and pressure are continuous. Consequently, the outgoing waves of a shock interaction are determined in the (u, P) -plane by the intersection of the right facing wave curve based on the right state and the left facing wave curve based on the left state. For example, in the collision of two shocks of the opposite wave family, the right state is the state behind the left incoming wave and the left state is the state behind the right incoming wave.

The non-degenerate wave families in two dimensions correspond to waves which rotate the flow direction either clockwise or counter-clockwise. For a stationary oblique shock the rotation of the streamline is referred to as the turning angle or deflection angle and is denoted by θ . Across a contact the pressure and normal velocity are continuous. In the distinguished frame in which the node (the intersection point of the shocks) is at rest, the normal velocity of the contact vanishes and the flow direction is continuous across the contact. Consequently, the outgoing waves are determined by the intersection of wave curves in the (θ, P) -plane. The shock portion of the wave curve in the (θ, P) -plane is referred to as the shock polar.

3.1. Interactions in one dimension

Next we discuss the consequences of the velocity bound, Theorem 3, for one-dimensional shock interactions. First we consider the collision of two shocks of the opposite wave family and show that the two outgoing waves must be shocks. The wave curves in the (u, P) -plane and the corresponding wave diagram in the (x, t) -plane are sketched in figure 3. Before the collision there is an incoming left facing shock 0-1_L and an incoming right facing shock 0-1_R. In order to prove that the outgoing waves are always shocks, we must show that the wave curve for an outgoing shock does not cross the wave curve for an incoming shock as shown in figure 4.

From figure 3, for right facing waves the condition that the wave curves do not cross is $u_{2_R} < u_{2'}$. This can be expressed in terms of the change in velocity across the three shocks, 0-1_R, 1_R-2_R and 0-2', as

$$|u_2 - u_1| - |u_1 - u_0| < |u_{2'} - u_0|, \tag{3.1}$$

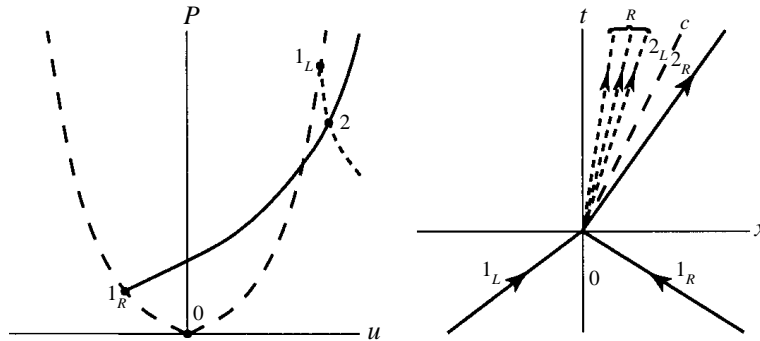


FIGURE 4. Excluded case in which the collision of two shocks of the opposite family would result in a reflected rarefaction.

where to simplify the notation we have denoted states 1_R by 1 and 2_R by 2. Since $|u_2 - u_1| - |u_1 - u_0| < |u_2 - u_1|$ and inequality (2.26) implies that $|u_2 - u_1| < |u_{2'} - u_0|$, condition (3.1) is satisfied. Hence the wave curves do not cross and the outgoing waves are always shocks.

Next we consider the collision of two shocks of the same wave family. The wave curves corresponding to the incoming shocks can cross in the (u, P) -plane as illustrated in figure 5. In particular, there may be a region on the second wave curve for which

$$|u_2 - u_1| + |u_1 - u_0| > |u_{2'} - u_0|,$$

even though by Theorem 3

$$(u_2 - u_1)^2 + (u_1 - u_0)^2 < (u_{2'} - u_0)^2.$$

As a consequence, there are two possible outcomes when one shock overtakes another. There is always a stronger transmitted shock of the same wave family, but either a reflected rarefaction or a reflected shock of the opposite wave family. These two cases have been previously noted by von Neumann (1945) and Fritz (1996). Typically, the reflected wave is a rarefaction. In the case with two shocks, Theorem 3 implies that the reflected shock is very weak compared to the transmitted shock.

When the outgoing waves are both shocks, there are two categories of particle paths, see figure 5(c). Paths in one set cross the two incoming shocks and the reflected outgoing shock (opposite wave family to the incoming shocks), while paths in the other set cross only the transmitted shock (same wave family as the incoming shocks). The boundary between these two sets of paths corresponds to a contact since Corollary 3 with $N = 3$ implies that the entropy behind the transmitted shock is higher than the entropy behind the reflected shock.

3.2. Interactions in two dimensions

In two dimensions, sequences of oblique shocks commonly occur in wave patterns resulting from shock interactions. The simplest examples for which the triple-shock entropy theorem apply are illustrated in figure 6. The shock waves in these patterns can be classified as incoming or outgoing (Landau & Lifshitz 1959, chap. X, § 102). The classification is according to the direction in which information flows. A wave is incoming if the component of the velocity in the direction of the front points towards the node, otherwise the wave is outgoing. Typically, two incoming shocks interact giving rise to two outgoing waves (shock or rarefaction) separated by a contact, see e.g. Glimm *et al.* (1985). Degenerate cases, in which one of the outgoing waves has

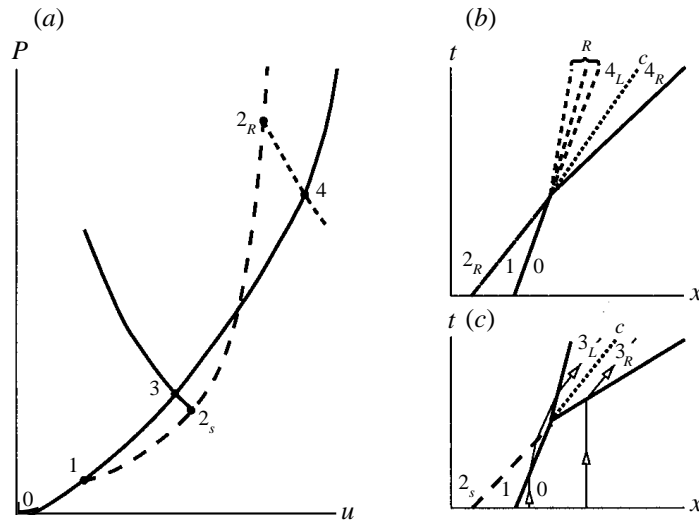


FIGURE 5. The interaction (overtake) of two shocks of the same wave family. (a) Hugoniot loci in the (u, P) -plane. (b) (x, t) -wave diagram when outgoing waves consist of reflected rarefaction and transmitted shock. (c) (x, t) -wave diagram when outgoing waves are both shocks. Thin lines with arrows represent particle paths.

zero strength and disappears, are important when the flow across a wave pattern is transonic. In the figure, an arrow on a shock front pointing towards the node indicates an incoming wave while an arrow pointing away from the node indicates an outgoing wave. The same convention is used in figures 3 and 4 to indicate incoming and outgoing waves in one dimension.

An exceptional case is the Mach reflection (MR) shown in figure 6(a). It consists of one incoming wave splitting into two outgoing waves and a contact. As discussed in a later subsection, this wave splitting does not cause a shock wave to be unstable. A consequence of the two-dimensional stability is that a Mach reflection with a reflected centred rarefaction does not occur.

A degenerate cross-node (DCN) is illustrated in figure 6(b). Superficially, this system looks like a Mach reflection and is sometimes referred to as an inverted Mach reflection (Courant & Friedrichs, 1948; Hornung 1986); but there are significant differences. First, it has two incoming shocks while the MR has only one. The extra incoming shock belongs to the opposite wave family than the Mach stem in a MR. Secondly, this reflection requires an extra boundary condition to generate the second incoming shock, e.g. a downstream blunt body as sketched or a downstream sonic choke. Thirdly, the contact is directed away from the wall while in MR it impacts on the wall. A cross-node usually has two outgoing waves. In the degenerate case, one outgoing wave has zero strength. Despite the degeneracy, this wave pattern can generically occur because the flow behind the second incoming wave is subsonic. Consequently, the shock front can curve in response to downstream boundary conditions and compensate for the lower-dimensionality of the degenerate wave pattern.

An overtake node also has two incoming shocks, but now they belong to the same wave family rather than the opposite family as in the cross-node. A degenerate overtake node (DON) is illustrated in figure 6(c). The outgoing waves consist of a transmitted shock and a contact. This only occurs when the flow downstream of the second incoming shock is subsonic. In the general case, the downstream flow

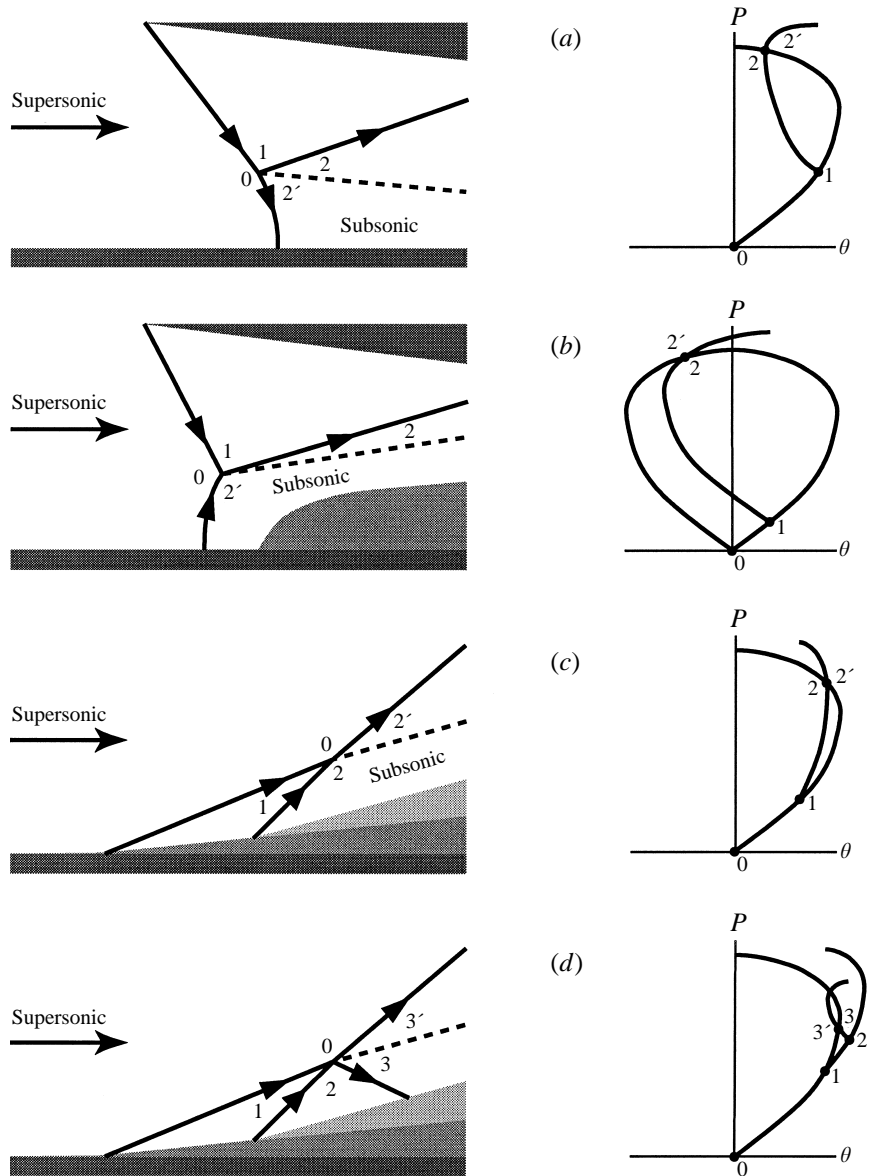


FIGURE 6. Examples of two-dimensional wave patterns: (a) Mach reflection, (b) degenerate cross-node, (c) degenerate overtake node, (d) overtake node with two outgoing shocks.

is supersonic and the overtake node gives rise to two outgoing waves separated by a contact; the extra wave may be either a shock, as shown in figure 6(d), or an expansion (not illustrated). The overtake node with two outgoing shocks is analogous to the one-dimensional shock interaction shown in figure 5(c).

We consider in detail a Mach configuration. As shown in figure 7, streamlines either go through the incident and reflected shocks, or through the Mach stem. Downstream of the node (triple point), pressure is continuous. The triple-shock entropy theorem implies that the entropy behind the Mach stem is higher than the entropy behind the reflected shock. Therefore, the intersection of three shocks *must* generate a contact.

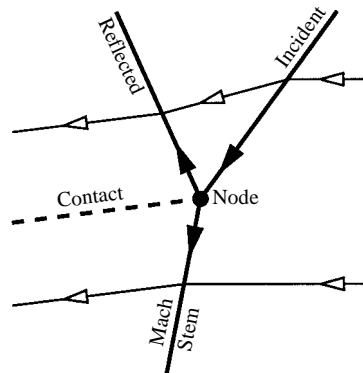


FIGURE 7. Streamlines for a Mach configuration in the rest frame of the node.

Weak reflections sometimes have the appearance, due to limited resolution, of three shocks intersecting without a contact. These patterns actually correspond to a von Neumann reflection (Colella & Henderson 1990) in which the node is smeared out and is not a singular point.

For a stationary wave pattern, the total enthalpy $\frac{1}{2}|\mathbf{u}|^2 + H$ is constant. By Corollary 4 the enthalpy is higher behind the Mach stem. Therefore, in the rest frame of the node, the velocity is lower behind the Mach stem than behind the reflected wave. Thus, at the contact in a Mach configuration there must be both an entropy jump and a velocity jump. Since the velocity jump occurs in the tangential component of the velocity, the contact is a velocity shear layer and a Mach configuration generates vorticity. The same considerations apply to the other examples shown in figure 6.

4. Non-uniqueness and hysteresis

When an equation of state is convex and satisfies the modified medium condition, along the Hugoniot locus both P and u are monotonic and extend to infinity. Moreover, the wave curves used in the analysis of the solution to a one-dimensional Riemann problem have a unique intersection, see e.g. Menikoff & Plohr (1989). Consequently, the outgoing waves that arise from a shock interaction in one dimension are unique.

In contrast to one-dimensional wave curves, shock polars are bounded and not monotonic. Consequently, in the graphical analysis of two-dimensional shock interactions the wave curves may have no intersection or more than one intersection. The case with multiple intersections is similar to what occurs in one dimension when the EOS is non-convex. Analogies with the non-convex one-dimensional case are noted later. When there is no intersection, the problem of non-existence is resolved with more complex wave patterns, either with transonic curved shocks or with composite wave patterns. Examples of the first type are von Neumann reflection (Colella & Henderson 1990), and anomalous reflection (Grove & Menikoff 1990). These wave patterns are not steady but may be pseudo-steady. Thus, resolution of non-existence may require time-dependent solutions. Composite wave patterns consist of multiple simple nodes separated by smoothly varying flow. The multiple nodes are a result of internal shocks generated by the incoming waves. Since the nodes have different velocities, the analysis of each simple node requires a different set of incoming and outgoing shock polars. Examples of composite wave patterns include complex Mach

reflection, double Mach reflection and the precursor wave pattern studied by Henderson, Colella & Puckett (1991). An analogous situation occurs in one dimension for a non-convex EOS. A rarefaction curve ends when $\mathcal{G} = 0$, and in order for all Riemann problems, i.e. shock interactions, to have a solution it is necessary to continue the rarefaction curve with a composite consisting of a rarefaction followed by an anomalous (entropy-increasing expansive) shock and then a second rarefaction, see Zel'dovich & Raizer (1967, chap. XI, §20). In this section, we only consider the problem of multiple intersections of the shock polars and the question it raises for non-uniqueness of shock interactions.

Let us consider a time-dependent problem in which the incoming wave types are assumed to be known at the initial time. When the solution changes slowly in time the wave pattern is determined by continuity of the polar solution. Some solutions have wave patterns in which the flow behind an outgoing wave is subsonic. In these cases, downstream boundary conditions are needed to determine the rest frame of the node. Time-dependent boundary conditions can cause a wave pattern to bifurcate or change form. Bifurcations can be triggered by acoustic waves impacting a node (the limiting case in which a weak node collides and scatters off another node) or forced by a sudden change in geometry, e.g. a shock impacting a wedge. Both shock tube experiments and numerical simulations have shown that when a shock impacts a wedge leading to a Mach reflection, the path of the triple point can be greatly affected by a boundary layer due to either viscosity or heat conduction (Henderson, Crutchfield & Virgona 1997). Thus, dissipative mechanisms at small scales can lead to local downstream boundary conditions which affects the bifurcation process. A bifurcation can only result in a wave pattern allowed by the shock polar analysis. Consequently, a wave pattern can bifurcate only when there is another local wave pattern compatible with shock polar analysis.

Additional complications arise when determining the wave patterns that occur in steady-state flows. In steady state, the wave pattern must be compatible with the global flow. Moreover, the identification of incoming and outgoing waves may depend on the downstream flow; e.g. figure 6(b) indicates how a downstream obstacle can lead to a degenerate cross-node in place of a more common regular reflection. Furthermore, the number of boundary conditions for the spatial region of interest depends on the nature of the flow, in particular, the number of families of characteristics that are directed into the region. Frequently, the downstream boundary conditions are not completely known ahead of time. For example, a vacuum pump may determine only the pressure or average flow rate in the downstream portion of a wind tunnel. As a local condition, this may not be sufficient to determine whether the outflow is supersonic or subsonic. Hence the number of incoming characteristics and the corresponding value of the Riemann invariants must be determined as part of the global solution. Consequently, the wave patterns are not always known *a priori*.

Hysteresis observed in experiments leading to steady-state flow shows that more than one global solution is compatible with the applied boundary conditions. In principle, the transients at the start of an experiment and the small-scale dissipative mechanisms (such as viscosity or heat conduction which can lead to boundary layers) determine the asymptotic steady-state flow. Without knowing the time history or the details of the dissipative mechanisms, the local stability of possible wave patterns is an important means for selecting which steady wave pattern is most likely to occur.

Next we analyse the stability of a planar shock wave in multi-dimensions. Similar considerations can be applied to resolve the non-uniqueness of shock polar solutions

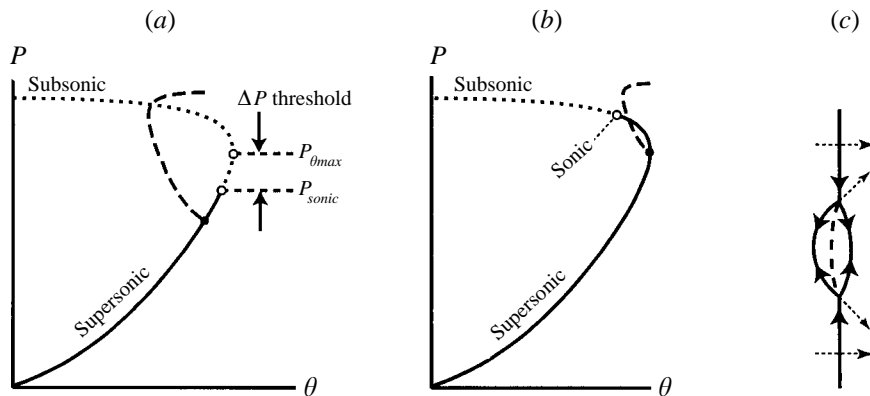


FIGURE 8. Two-dimensional shock splitting. (a) Pressure threshold when two-dimensional stability condition holds. (b) Shock polars when the stability condition is not satisfied. (c) Shock front with a pair of Mach nodes that spontaneously form when the two-dimensional stability condition is violated. Dotted lines with arrows indicate the direction of propagation of the shock fronts and of each node.

that arise in many applications. This also leads to the idea of a stability threshold which provides an explanation of when and why hysteresis can occur.

4.1. Stability

One example of non-uniqueness is the possibility of shock splitting, i.e. a Mach configuration represents an incoming shock splitting into two outgoing shocks, see figure 6(a). If this splitting were to occur spontaneously then a shock wave would be unstable. The linear stability analysis by Kontorovich (1959) can be used to determine the conditions for which a planar shock wave is stable to two-dimensional perturbations. Fowles (1981) showed that the shock stability condition can be expressed simply as an algebraic condition involving the equation of state and the pressure ahead of and behind the shock

$$(\Gamma + 1) \frac{\Delta P}{P} < \gamma. \quad (4.1)$$

When the equation of state satisfies the two-dimensional stability condition, $\Gamma + 1 \leq \gamma$, all pressure increasing shocks are two-dimensionally stable. Moreover, as derived in Appendix B, Fowles showed that the stability inequality is equivalent to a geometric condition on a shock polar, namely the sonic point occurs at a lower pressure than the maximum turning angle. As a consequence there is a minimum strength for the reflected wave in a Mach configuration since on the shock polar, see figure 8(a), the ahead state lies below the sonic point and the behind state lies above the maximum turning angle. We next show that the minimum reflected wave strength can be interpreted as giving rise to a non-zero threshold for a perturbation to cause a shock to split.

Let us consider a shock wave for which the stability condition is violated. A continuous path can be constructed by which a shock can split into two shocks with a higher entropy as follows. We choose the reference frame in which the shock front is stationary and the incoming velocity is given by (B 2). In this frame the shock corresponds to the detachment point on the shock polar. By Theorem 6 (in Appendix B) the detachment point is supersonic. If the tangential component of the incoming velocity is increased slightly then the shock state remains supersonic

but lies slightly below the detachment point on the new shock polar as shown in figure 8(b). Consequently, the shock can split into a pair of Mach configurations, see figure 8(c), in which the Mach stem has only a slightly greater shock pressure and the reflected wave is arbitrarily weak. By slowly increasing the tangential component of the incoming velocity (in effect, this varies the node velocity), there is a continuous path in which the reflected shock increases in strength. It follows from the triple-shock theorem that the shock splitting raises the entropy of the flow. This simple picture underlies the weakly nonlinear analysis of Majda & Rosales (1983).[†]

Both Kontorovich (1959) and Fowles (1981) presented an alternative way of viewing the instability. Consider a shock interaction in which one of the incoming waves is weak, i.e. an acoustic wave. An important parameter characterizing the interaction is the reflection coefficient; the ratio of the pressure jump across the reflected wave to the pressure jump across the weak incoming wave. If the stability condition is violated, then there is an angle of incidence between the shock and the weak wave such that the reflection coefficient is infinite. This angle of incidence corresponds to the reference frame in which the shock state coincides with the detachment point on the shock polar. The infinite reflection coefficient implies that an arbitrarily weak perturbation leads to a finite outgoing wave. Consequently, the outgoing waves are spontaneously formed and the shock front is unstable leading to transverse waves propagating along the shock front. A similar transverse instability has been observed experimentally and numerically for detonation waves; see e.g. Fickett & Davis (1979) and references therein and Bourlioux & Majda (1992). However, the instability of the detonation wave depends on the reaction zone dynamics and is not merely the result of violating the stability condition for the equation of state of the reaction products; see also Mond & Rutkevich (1994) for the derivation of a modified stability condition applicable to a partly dispersed shock in which the relaxation is due to ionization.

Conversely, when the stability condition holds there is no continuous path along which a shock wave can split into a higher entropy state. The stability condition can be interpreted as giving rise to a threshold. Waves with an amplitude below the threshold are scattered from a shock front (the analogue of elastic scattering) while waves above the threshold cause a bifurcation of the shock front in which a pair of Mach nodes are formed (the analogue of inelastic scattering).

Next we discuss the transition between regular and Mach reflection. There is a range in parameter space (shock strength and incident shock angle) for which a symmetric pair of incoming shocks can give rise, based on shock polar analysis, to either regular reflection (cross-node) or Mach reflection (pair of Mach nodes). A transition criterion is frequently used to resolve the non-uniqueness in the wave pattern. Many steady-state wind tunnel and shock tube experiments have shown that if the flow is two-dimensional then the transition criterion for strong incident waves corresponds to the von Neumann or mechanical equilibrium point on the shock polar (Molder 1971; Pantazapol Bellet & Soustre 1972; Henderson & Lozzi 1975; Hornung *et al.* 1979; Hornung & Robinson 1982).

In the wind tunnel experiments, see figure 9, the incoming flow velocity is fixed and the shock waves are generated by wedges placed in the flow stream. As the wedge angle is varied the state behind the lead (upstream) shock moves along a fixed shock

[†] Majda & Rosales (1983) attempted to explain the transverse instability observed experimentally in propagating detonation waves. Their analysis neglected the dynamics of the reaction zone by treating the detonation wave as a discontinuity. Consequently, their analysis really applies to shock waves rather than detonation waves.

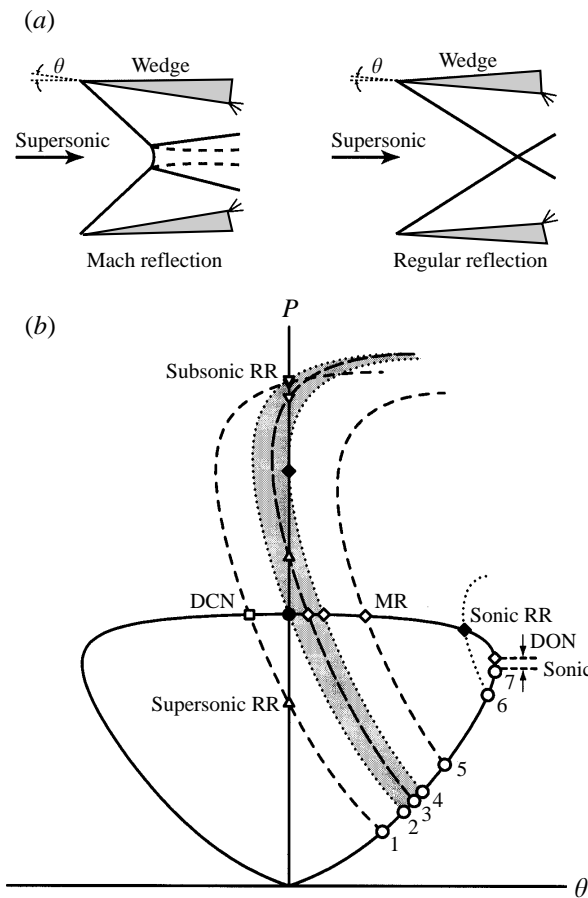


FIGURE 9. Hysteresis effect for transition between regular reflection and Mach reflection. (a) Wind tunnel experiment in which hysteresis is observed. The wedges can be rotated about the upstream corner to vary incoming shock waves. (b) Shock polar diagram for the wave pattern generated by experiment. The polar for the incoming wave is shown as a solid line and the polar for the reflected wave as a dotted or dashed line. The symbols denote the following wave states: \circ an incoming shock state; \triangle a supersonic regular reflection (RR) state; ∇ a subsonic RR state; \diamond , a Mach reflection (MR) state; \square , a degenerate cross-node (DCN) state; \bullet , is the von Neumann (mechanical equilibrium) transition point; \blacklozenge , either the detachment transition point or the point at which the reflected wave in Mach configuration becomes subsonic. Horizontal dashed lines bound the small region for degenerate overtake node (DON) states. The reflected polars with both RR and MR comprise the shaded region.

polar. At some angle the reflected shock polar intersects the incident shock polar at its maximum pressure. This intersection point is known as the von Neumann or mechanical equilibrium point. For smaller wedge angles the incoming shock pressure is lower and only regular reflection is possible, while at larger angles both regular and Mach reflection are possible. At the von Neumann point, the pressure immediately downstream of the shock intersection point is the same for both regular and Mach reflection. The triple-shock theorem implies that the Mach configuration has a higher entropy than that of the regular reflection. By continuity, in the neighbourhood of the mechanical equilibrium point, the Mach configuration still has the higher entropy. For a continuous transition one expects the higher entropy configuration would be

favoured based on thermodynamic stability. This provides a heuristic motivation for the von Neumann point as the transition criterion.

A similar non-uniqueness occurs in one dimension when the equation of state is non-convex. In some limited regimes in phase space, both a single shock wave and a composite wave, consisting of a sonic shock followed by a compressive wave, can have the same final pressure. We note that a compressive wave can spread out rather than focusing into a shock in regions of phase space with $\mathcal{G} < 0$. The non-uniqueness is resolved with the Oleńnik-Liu extended entropy condition Liu (1976a); accordingly shock waves on the Hugoniot locus for which there exists a shock with a lower pressure and a larger shock speed are excluded and replaced by composite waves. Liu (1976b) showed that the extended entropy condition selects those shocks corresponding to the solution of the fluid equations with vanishing viscosity. The admissible waves can also be justified with a stability argument; namely, perturb the shock by smearing it into a smooth profile and then analyse the evolution of the profile by examining how the characteristics focus to regenerate the shock wave. The extended entropy condition is equivalent to selecting the wave, single shock or composite, which for a given pressure has the higher entropy.

4.2. Hysteresis

In the region in which the solution to the shock polars is not unique, hysteresis has been observed both experimentally and numerically for the regular to Mach transition: see Chpoun *et al.* (1995), Vuillon, Zeitoun & Ben-Dor (1995), Ivanov *et al.* (1995a, b), Henderson *et al.* (1997). To set the stage for our discussion of the transition we first describe the possible wave patterns derived from shock polar analysis. The shock polar diagram corresponding to the quasi-steady wind tunnel experiments is shown in figure 9. This particular diagram is for an ideal gas EOS with $\gamma = 1.4$ and an incident flow Mach number of 3.5. (The structure would be qualitatively different only for a low incident Mach number.) There are several distinct regimes:

(1) *Regular reflection only* (state 1). At small wedge angles the incident shock has low pressure and there are three possible wave patterns: (i) supersonic regular reflection, (ii) degenerate cross-node, (iii) subsonic regular reflection. The degenerate cross-node is not admissible since it has two incoming waves and the flow can only support one. This is because the contacts behind the DCN would form a diverging nozzle. Since the flow is subsonic the pressure would have to increase. But the downstream boundary condition does not support the pressure increase. Hence the degenerate cross-node cannot occur in the steady flow. The subsonic regular reflection is unstable to small perturbations (Teshukov 1989). Therefore, it cannot occur in the asymptotic steady state flow. Consequently, in this regime only the supersonic regular reflection occurs.

(2) *Von Neumann (mechanical equilibrium) point* (state 2). For a particular incoming shock strength, the supersonic RR coincides with the maximum pressure on the incident shock polar. This is the transition between the DCN in the previous case and the MR in the next case.

(3) *Regular reflection and Mach reflection* (state 3). Immediately above the von Neumann point (slightly stronger incident shock wave) both supersonic regular reflection and Mach reflection are possible. The reflected wave in the Mach configuration is supersonic. Again the subsonic regular reflection is inadmissible based on stability.

(4) *Sonic regular reflection*. As the incident shock strength increases a point is reached at which the regular reflection becomes sonic. For stronger incident shocks both regular reflection solutions are subsonic.

(5) *Detachment point* (state 4). There is a distinguished incident shock strength at which the two possible regular reflections coalesce. The regular reflection is subsonic. For stronger incident shocks there are no regular reflection shock polar solutions.

(6) *Mach reflection only* (state 5). The shock polar diagram has a unique solution corresponding to Mach reflection. The reflected wave in the Mach configuration is supersonic.

(7) *Mach reflection with sonic reflected wave* (state 6). As the incident shock strength increases a point is reached at which the reflected wave in the Mach configuration becomes sonic. For stronger incident shocks the reflected wave is subsonic.

(8) *Termination point for Mach reflection* (state 7). As the incident shock strength is further increased a point is reached at which the deflection angle vanishes for the reflected wave in the Mach configuration. This is the termination point of the Mach wave patterns.

(9) *Degenerate overtake node*. For still larger incident shock strength, the shock polar diagram has a unique solution corresponding to a degenerate overtake node. This wave pattern is not admissible since it has two incoming waves and the flow can support only one incoming wave. Most likely, the flow pattern will have a single curved shock wave which begins at the tip of one wedge and ends at the tip of the other wedge. A similar curved shock occurs in the pseudo-steady case; (Hornung 1986, figure 13). For weak incident shocks this becomes the von Neumann reflection (Colella & Henderson 1990).

(10) *Beyond maximum turning angle*. When the wedge angle is greater than the maximum turning angle on the incident shock polar, no shocks in the channel between the wedges are possible. A bow wave will develop in front of the wedges leading to subsonic flow in the channel.

Downstream boundary conditions and stability are determining factors in selecting admissible steady-state wave patterns. However, in regime (3) there still remains two possibilities: either regular reflection or Mach reflection. We note that Hornung (1986) presented a similar catalogue of wave patterns for the pseudo-steady flow that occurs in shock tube experiments studying the impact of a shock on a wedge. In the shock tube experiments, the shock strength is fixed and the wedge angle is varied. In this case the incident wave speed in the frame of the node is not fixed. Consequently, the different regimes cannot be pictured on a single-shock polar diagram.

For the wind tunnel experiments the incoming flow velocity is fixed and the wedge angle is slowly varied. The wave pattern is quasi-steady but changes with the wedge angle. Some of the experiments show the following hysteresis effect. At small wedge angles there is only one allowed wave pattern and regular reflection is observed. As the wedge angle is increased and the incident pressure rises above the von Neumann point, the regular reflection is maintained. Beyond the detachment point regular reflection is not possible and the pattern abruptly changes to Mach reflection. Then as the wedge angle decreases the Mach reflection continues to occur until the von Neumann point. Thus, with increasing wedge angle the transition from regular to Mach reflection occurs near the detachment point while with decreasing wedge angle the transition from Mach to regular reflection occurs at the von Neumann point. Other experiments do not show a hysteresis effect and both transitions occur at the von Neumann point.

The hysteresis effect implies that both configurations are locally stable. Several experiments suggest that the transition is affected by the flow behind the node as follows.

- (i) When a shock reflects from a curved wall, the transition angle varies with the

shape of the wall (Henderson & Lozzi 1979; Ben-Dor, Takayama & Kawauchi 1980; Takayama & Sasaki 1983).

(ii) Both regular and Mach reflection occur simultaneously when a planar shock impacts a cylindrical cone whose axis is not aligned with the shock normal. The angle between the shock and the cone wall varies with the azimuthal angle of the cone, and at some angle the wave pattern changes from regular to Mach reflection. The transition angle along the cone is not the same as for a planar wedge (Suzuki, Sakamura & Yin 1995; Yang, Sasoh & Takayama 1996).

(iii) Cylindrically or spherically converging shocks appear to become unstable to transverse waves (i.e. Mach configurations spontaneously form) at large convergence ratios when the flow gradients behind the shock front becomes large (Wallus & Demmig, 1995).

To understand this phenomenon, we suggest an analogy with a gas/liquid phase transitions. The following are the relevant aspects of a phase transition. The constraints of the system require that in equilibrium the two phases have the same pressure and temperature. Long-lived meta-stable states can exist, such as a super-cooled gas. The lifetime of the meta-stable state can be greatly diminished by impurities such as nucleation centers. This is because there is a potential barrier between a super-cooled gas and a liquid. Surface energy at a gas/liquid interface causes small drops formed by thermodynamic fluctuations to be thermodynamically unfavourable and to evaporate before they can grow into the stable equilibrium state. A nucleation site decreases the potential barrier and increases the rate at which large drops form.

For the analogy we have in mind the two wave patterns, Mach reflection and regular reflection, play the role of the two phases. In steady-state flow, the total enthalpy is a constant. The equilibrium configuration is determined by maximizing the entropy subject to the constraint that both the pressure and the total enthalpy are fixed. By the triple-shock theorem, the Mach reflection corresponds to the equilibrium state and the regular reflection to a meta-stable state.

The hysteresis effect for the regular to Mach transition may be explained by the hypothesis that there is a transition threshold. Acoustic noise sets the background perturbation amplitude and is the analogue of thermodynamic fluctuations. A flow gradient or a boundary layer (Henderson *et al.* 1997) along the wedge wall affects the transition threshold and plays a role similar to that of a nucleation centre on the potential barrier. The lifetime of the meta-stable regular reflection configuration can be decreased causing a transition to the maximum entropy Mach reflection either by lowering the threshold or by raising the background noise. Conversely, the transition can be delayed by either raising the threshold or by lowering the background noise. Only when perturbations are below the threshold would hysteresis be observed (Ivanov *et al.* 1995*b*). Without flow gradients to raise the threshold, there is usually sufficient noise in a wind tunnel for the most stable local configuration to occur. This is compatible with the many experiments that measure the transition between regular and Mach reflection to occur at the von Neumann point.

An important source of flow gradients are from three-dimensional effects; for example, when a shock impacts a cone at an angle of attack, the transverse gradient is from the asymmetry of the conical flow and as noted previously this affects the transition. In recent experiments with open sided models (Chpoun *et al.* 1995; Fomin *et al.* 1996; Skews, 1996) there are transverse gradients that have a decisive influence on the hysteresis effect. In particular, if the aspect ratio, height to width of the model inlet, is greater than 2.5 then transition occurs at the von Neumann point. In this case the transverse gradients are small and have no effect on transition and there

is no hysteresis. However, if the aspect ratio is reduced to 1 or less then there is a significant hysteresis effect.

In summary, when the local analysis of a shock interaction has more than one solution, the non-uniqueness is resolved by considering the stability of the solution. Local stability suffices to determine uniquely the wave structure in many cases. Common examples in two dimensions include the cases when the possible outcomes are (i) supersonic versus subsonic regular reflection, and (ii) regular reflection versus inverted Mach reflection. When more than one solution is locally stable, other considerations such as global boundary conditions are needed. In some cases, the boundary conditions are such that hysteresis can occur. Regular versus Mach reflection is an example of this case. Transition criteria are then inadequate and the concept of a transition threshold becomes important. When there is sufficient noise in the system, the highest entropy solution appears to be most stable and would occur. For the transition between regular and Mach reflection, the triple-shock entropy theorem then leads to the mechanical equilibrium transition criterion for the most favoured wave pattern. Analogies with meta-stable thermodynamic states and phase transitions are helpful in understanding the possible transitions when the outcome of a shock interaction is non-unique.

This research is supported by the US Department of Energy, Los Alamos National Laboratory.

Appendix A. Implicit value theorem

Our proof that the Hugoniot locus for a convex equation of state can be parameterized by the entropy, Corollary 1, depended critically on the implicit value theorem. This theorem is a corollary of the inverse function theorem. Here we state a simple version of the theorem sufficient for our needs.

THEOREM 4 (INVERSE FUNCTION THEOREM). *Suppose that the function $\mathbf{f}: \mathbb{R}^n \rightarrow \mathbb{R}^n$ is continuously differentiable. Let $\mathbf{f}'(a)$ denote the derivative of \mathbf{f} at a , i.e. the matrix of partial derivatives. If $\det \mathbf{f}'(a) \neq 0$ then there are open sets V and W such that $a \in V$ and the restriction $\mathbf{f}: V \rightarrow W$ has a continuous inverse $\mathbf{f}^{-1}: W \rightarrow V$ that is differentiable.*

For an elementary proof, see for example, Spivak (1965, p. 35).

For our application to the Hugoniot locus we define the function from $\mathbb{R}^2 \rightarrow \mathbb{R}^2$ by $\mathbf{f}(P, S) = (\tilde{h}(P, S), S)$. The derivative matrix is given by

$$\mathbf{f}' = \begin{pmatrix} \partial_P \tilde{h} & 0 \\ \partial_S \tilde{h} & 1 \end{pmatrix}.$$

It follows that $\det \mathbf{f}' = \partial_P \tilde{h}$. Therefore, the inverse function theorem applies when $\partial_P \tilde{h} \neq 0$, and then locally $P = P(\tilde{h}, S)$. Since the Hugoniot locus is defined by $\tilde{h} = 0$, there is then a neighbourhood of a point on the Hugoniot locus in which $P_h = P(0, S)$. Because P and S are sufficient to define the state behind the shock front, the Hugoniot locus is locally parameterized by S about any point at which $\partial_P \tilde{h} \neq 0$. This is an example of how the equation $\tilde{h}(P, S) = 0$ implicitly defines a function $P_h(S)$ when one of the partial derivatives (in this case $\partial_P \tilde{h}$) is non-zero.

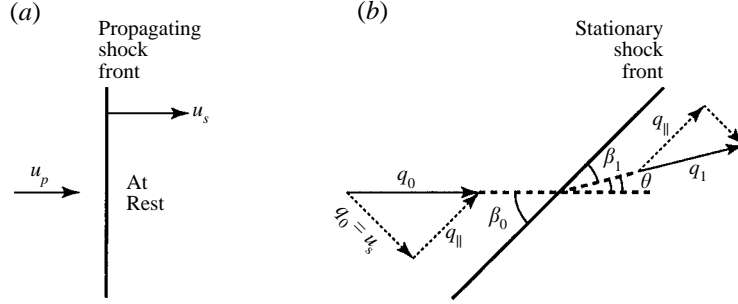


FIGURE 10. Notation used to describe velocities across shock front. (a) one-dimensional (normal) shock wave in the rest frame of the state ahead of the shock front. (b) Oblique two-dimensional shock wave in the rest frame of the shock front.

Appendix B. Detachment and sonic points on a shock polar

A shock polar describes the properties of stationary oblique shocks used in the analysis of two-dimensional wave patterns. For a given upstream state, the shock polar relates the downstream pressure to the deflection angle of a streamline through the shock front. It plays a similar role for determining the outcome of two-dimensional shock interactions as the projection of the Hugoniot locus in the (u, P) -plane does for the solution of a one-dimensional Riemann problem.

In this section, the properties of a shock polar are derived which we use in our analysis of two-dimensional shock stability. First, we relate the shock polar to the Hugoniot locus. It is convenient to choose a reference frame for one-dimensional shock waves in which the flow ahead of the shock front is at rest, see figure 10(a). We denote by u_s and u_p the velocity of the shock front and the particle velocity behind the front, respectively. When $\mathcal{G} > 0$ and $\Gamma < \gamma$, either u_s or u_p may be used to parameterize the one-dimensional Hugoniot locus. Moreover, we consider only the physical entropy-increasing shocks. These are compressive and pressure increasing. For an oblique two-dimensional shock wave, we use the reference frame in which the shock front is at rest, see figure 10(b). We denote by q_0 the velocity ahead of the front, and β_0 and β_1 the angles between the shock front and the streamline ahead of and behind the front respectively. Since the flow ahead of the shock is supersonic, the shock polar is only defined for $q_0 > c_0$ and the angle of the front is restricted to the range $\sin^{-1}(c_0/q_0) \leq \beta_0 \leq \frac{1}{2}\pi$. The component of the velocity parallel to the front is denoted q_{\parallel} . It is continuous across the front. Hence, $q_{\parallel} = q_0 \cos(\beta_0) = q_1 \cos(\beta_1)$. The deflection angle of the streamlines is given by $\theta = \beta_0 - \beta_1$. As in one dimension, there are two non-degenerate wave families; oblique shocks with positive and negative deflection angle ($\theta > 0$ and $\theta < 0$) are the analogue of the left and right facing one-dimensional waves.

From the geometry in figure 10, the angles of the streamlines for an oblique shock are related to the one-dimensional shock velocities as follows:

$$\tan \beta_0 = \frac{u_s}{q_{\parallel}}, \quad \tan \beta_1 = \frac{u_s - u_p}{q_{\parallel}}.$$

Using the trigonometric identity for the tangent of the difference of two angles, we obtain

$$\begin{aligned} \tan \theta &= \frac{\tan \beta_0 - \tan \beta_1}{1 + \tan \beta_0 \tan \beta_1} \\ &= \frac{u_s u_p}{q_0^2 - u_s u_p} \cdot \frac{q_{\parallel}}{u_s}. \end{aligned} \tag{B 1}$$

At the detachment point of a shock polar, the deflection angle is maximum. It is determined by the condition

$$\frac{d}{du_p} \log \tan \theta = 0.$$

Straightforward algebra reduces this condition to the equation

$$q_0^2 = u_s^2 + (u_s - u_p)u_p \frac{du_s}{du_p}. \quad (\text{B } 2)$$

From (B 2) we can deduce

THEOREM 5. *Suppose $\mathcal{G} > 0$ and $\Gamma \leq \gamma$ are satisfied everywhere. Consider the one-parameter family of shock polars in which the upstream thermodynamic state (V_0, S_0) is fixed and q_0 is varied. Then the following conditions are equivalent:*

- (i) *on the Hugoniot locus based on the state (V_0, S_0) the quantity $u_s^2 + (u_s - u_p)u_p du_s/du_p$ is monotonically increasing with increasing shock strength;*
- (ii) *every shock coincides with the detachment point on a shock polar for a unique value of q_0 ;*
- (iii) *every shock polar has a unique local extremum in θ , and hence one and only one detachment point.*

COROLLARY 5. *Suppose $\mathcal{G} > 0$ and $\Gamma \leq \gamma$ are satisfied everywhere. Consider the Hugoniot locus based on the thermodynamic state (V_0, S_0) . If on the Hugoniot locus*

$$V_0 \frac{d^2 P}{du_p^2} + \frac{du_s}{du_p} > 0 \quad (\text{B } 3)$$

is satisfied, then every shock polar with the initial thermodynamic state (V_0, S_0) has a unique detachment point.

Proof. By differentiation of (B 2), the monotonicity condition in Theorem 5 is equivalent to

$$u_p \left(1 + \frac{du_s}{du_p} \right) \frac{du_s}{du_p} + (u_s - u_p) \left(u_p \frac{d^2 u_s}{du_p^2} + 3 \frac{du_s}{du_p} \right) \geq 0. \quad (\text{B } 4)$$

From the Hugoniot jump conditions

$$\Delta P = \rho_0 u_p u_s.$$

The second derivative of P is given by

$$V_0 \frac{d^2 P}{du_p^2} = u_p \frac{d^2 u_s}{du_p^2} + 2 \frac{du_s}{du_p}. \quad (\text{B } 5)$$

Substituting (B 5) into (B 4) we obtain

$$(u_s - u_p) \left(V_0 \frac{d^2 P}{du_p^2} + \frac{du_s}{du_p} \right) + u_p \left(1 + \frac{du_s}{du_p} \right) \frac{du_s}{du_p} \geq 0.$$

Since $u_s > u_p$ and $du_s/du_p > 0$, (B 3) is a sufficient condition for (B 4). \square

When the EOS satisfies $\mathcal{G} > 0$ and $\Gamma \leq \gamma$, the shock velocity is monotonically increasing, i.e. $du_s/du_p > 0$. Consequently, convexity of $P(u_p)$ is a sufficient condition for a unique detachment point. We note that convexity of wave curves, i.e.

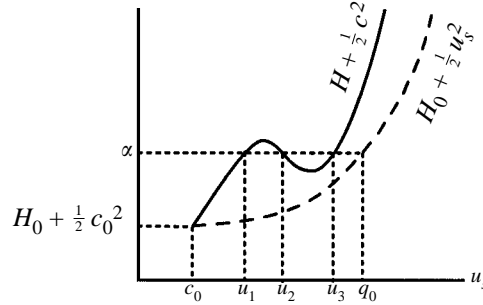


FIGURE 11. Sketch of functions used to show when a shock polar has a non-unique sonic point. The Hugoniot locus is parameterized by u_s . The solid line is the function $H + \frac{1}{2}c^2$ and the dashed line is the function $H_0 + \frac{1}{2}u_s^2$. A value of q_0 and the corresponding shocks for multiple sonic points are indicated.

$d^2P/du_p^2 > 0$, is also a sufficient condition to guarantee convergence when solving one-dimensional Riemann problems with a second-order Newton iteration algorithm.

The stability of shock waves in multi-dimensions is determined by the position on the shock polar of the sonic point relative to the detachment point. First, we determine the sonic point. In the rest frame of the shock front, the total enthalpy is a constant. Hence,

$$q^2 - c^2 = q_0^2 + 2H_0 - (2H + c^2), \tag{B 6}$$

where $H = e + PV$ is the specific enthalpy. From this we can deduce

LEMMA 4 (TESHUKOV 1986). *Suppose $\mathcal{G} > 0$ is satisfied everywhere. Consider the one-parameter family of shock polars in which the upstream thermodynamic state (V_0, S_0) is fixed and q_0 is varied. For all $q_0 > c_0$ the shock polars have a unique sonic point if and only if along the Hugoniot locus based on the state (V_0, S_0) the quantity $H + \frac{1}{2}c^2$ is monotonically increasing with shock strength.*

Proof. On the shock polar, the flow behind weak shocks, $\sin \beta_0 \gtrsim c_0/q_0$, is supersonic while the flow behind nearly normal shocks, $\sin \beta_0 \lesssim \pi/2$, is subsonic. By continuity there is at least one sonic point on every shock polar. If $H + \frac{1}{2}c^2$ is monotonic then by (B 6) $q^2 - c^2$ is monotonic and there is only one sonic point.

Since $\mathcal{G} > 0$, the Hugoniot locus may be parameterized by u_s . Figure 11 illustrates the case when $H + \frac{1}{2}c^2$ is not monotonic. Suppose the constant function $\alpha(u_s) = \alpha$ intersects the curve $H + \frac{1}{2}c^2$ more than once. We can choose q_0 such that $\alpha = H_0 + \frac{1}{2}q_0^2$. Since the flow behind a normal shock ($u_s = q_0$) is subsonic, the curve $H_0 + \frac{1}{2}u_s^2$ lies below and to the right of the curve $H + \frac{1}{2}c^2$. Therefore, the values of $(u_s)_i$ at which $H + \frac{1}{2}c^2 = \alpha$ are all less than q_0 , and the shock polar for q_0 has a sonic point at every intersection of α with the curve $H + \frac{1}{2}c^2$. Thus, if $H + \frac{1}{2}c^2$ is not monotonic then there is a q_0 such that the shock polar has more than one sonic point. \square

For weak shocks it can be shown from a Taylor expansion of the Hugoniot jump conditions that

$$c = c_0 + (\mathcal{G}_0 - 1)u_p + O(u_p^2), \quad u_s = c_0 + \frac{1}{2}\mathcal{G}_0 u_p + O(u_p^2).$$

Hence,

$$u_s^2 + (u_s - u_p)u_p \frac{du_s}{du_p} = c_0^2 + \frac{3}{2}\mathcal{G}_0 c_0 u_p + O(u_p^2),$$

$$H + \frac{1}{2}c^2 = H_0 + \frac{1}{2}c_0^2 + \mathcal{G}_0 u_p + O(u_p^2).$$

Therefore, for convex equations of state when the Mach number ahead of the shock is near 1, i.e. $0 < q_0/c_0 - 1 \ll 1$, shock polars have a unique detachment point and a unique sonic point.

More generally, after some algebra, it can be shown that along the Hugoniot locus

$$\frac{1}{T} \frac{d}{dS} (H + \frac{1}{2}c^2)_h = 1 + \Gamma + \gamma \left[\mathcal{H} + \mathcal{G} \left(\frac{-P}{T} \frac{dV}{dS} \right)_h \right], \quad (\text{B } 7)$$

where \mathcal{H} is another dimensionless parameter describing the equation of state

$$\mathcal{H} = \frac{1}{2\gamma} \left. \frac{\partial c^2}{\partial e} \right|_V,$$

and

$$\left(\frac{P}{T} \frac{dV}{dS} \right)_h = \frac{2V}{\Delta V} \left(\frac{1 + \frac{1}{2}\Gamma \Delta V/V}{\gamma + (V/P)(\Delta P/\Delta V)} \right)$$

measures the variation of V with entropy along the Hugoniot locus. (Teshukov 1986 obtained an alternative formulae but it is harder to interpret.) We note that \mathcal{H} is proportional to $\partial c^2/\partial T|_V$ and is typically positive. Moreover, V typically decreases with shock strength, i.e. $-dV/dS|_h > 0$, except when the Hugoniot locus goes through regions of phase space in which dissociation or ionization are dominant effects. Consequently, the right-hand side of (B 7) is typically positive and the Hugoniot locus typically satisfies the condition required for a shock polar to have a unique sonic point. Also, (B 4) is typically satisfied and shock polars typically have a unique detachment point.

Next we determine the relative positions of the sonic and detachment points. First we note that substituting the Hugoniot equation

$$2(H - H_0) = (V + V_0)\Delta P$$

into (B 6) we obtain for the sonic condition

$$q^2 - c^2 = q_0^2 - [\gamma P V + (V_0 + V)\Delta P]. \quad (\text{B } 8)$$

In order to evaluate (B 2) for the detachment point we need an expression for du_s/du_p . In their review article, Menikoff & Plohr (1989) have systematically determined the differential of all quantities along the Hugoniot locus. From their equations (4.26) and (4.27) we obtain

$$\frac{du_s}{du_p} = \frac{(\gamma + (V/P)(\Delta P/\Delta V)) V_0 m^2 / \Delta P}{\gamma - \Gamma \Delta P/P - (V/P)(\Delta P/\Delta V)}, \quad (\text{B } 9)$$

where $m^2 = -\Delta P/\Delta V = (\rho_0 u_s)^2$ is the square of the mass flux through the shock front. Substituting (B 9) along with the equations for the velocities

$$u_s = V_0 m, \quad u_p = (V_0 - V)m, \quad u_s - u_p = Vm,$$

into (B 2) and subtracting $\gamma P V + (V_0 + V)\Delta P$ from both sides of the equation we

obtain

$$q^2 - c^2 = V_0^2 m^2 - \gamma P V + (V_0 + V) \Delta P + \frac{(V_0 - V) V m^2 (\gamma + (V/P)(\Delta P/\Delta V)) V_0 m^2 / \Delta P}{\gamma - \Gamma \Delta P/P - (V/P)(\Delta P/\Delta V)}.$$

Simple algebraic manipulations reduces the equation for the detachment point to

$$(q^2 - c^2) \left(\gamma - \frac{\Delta P}{P} \Gamma + \frac{V}{P} m^2 \right) = -P V \left(\gamma - \frac{V}{P} m^2 \right) \left[\gamma - \frac{\Delta P}{P} (\Gamma + 1) \right]. \quad (\text{B } 10)$$

We can now derive an important property of a shock polar.

THEOREM 6 (FOWLES 1981). *Suppose $\mathcal{G} > 0$ and $\Gamma \leq \gamma$ are satisfied everywhere. On a shock polar the detachment point is subsonic if and only if*

$$\frac{\Delta P}{P} (\Gamma + 1) < \gamma. \quad (\text{B } 11)$$

Proof. We consider the sign of the factors on the left- and right-hand sides of (B 10). Since the physical shocks are pressure increasing, $0 < \Delta P/P < 1$. From the condition $\Gamma \leq \gamma$, it follows that $\gamma - (\Delta P/P)\Gamma + (V/P)m^2 > 0$. Moreover, the state behind a physical shock is subsonic. Hence, $P V [\gamma - (V/P)m^2] = c^2 - (u_s - u_p)^2 > 0$. Therefore, the sign of $c^2 - q^2$ is the same as the sign of $\gamma - (\Delta P/P)(\Gamma + 1)$. Consequently, the detachment point is subsonic, $c > q$, if and only if (B 11) is satisfied. \square

COROLLARY 6. *Suppose $\mathcal{G} > 0$ and $\Gamma + 1 \leq \gamma$ are satisfied everywhere. If a shock polar has a unique sonic point and a unique detachment point then in the (θ, P) -plane the detachment point lies above the sonic point, i.e. the detachment point has a higher pressure than the sonic point.*

Proof. Points on the shock polar corresponding to weak shocks ($u_s \gtrsim c_0$) are supersonic while those corresponding to normal shocks ($u_s \lesssim q_0$) are subsonic. Since there is a unique sonic point on the shock polar, only those shocks with a pressure above the pressure at the sonic point are subsonic. By the previous theorem, the detachment point is subsonic. Therefore, it has a higher pressure than the sonic point. \square

As discussed in §4.1, inequality (B 11) is necessary for multi-dimensional shock stability. We note that since $\gamma > 0$, the inequality (B 11) is true for sufficiently weak shocks. Hence, weak shocks are always stable. For every shock to satisfy the multi-dimensional stability condition requires $\Gamma + 1 \leq \gamma$. This is stronger than the medium condition needed for uniqueness of all one-dimensional Riemann problems.

REFERENCES

- BEN-DOR, G., TAKAYAMA, K. & KAWAUCHI, T. 1980 The transition from regular to Mach reflexion and from Mach to regular reflection in truly nonstationary flows. *J. Fluid Mech.* **100**, 147–160.
- BETHE, H. 1942 The theory of shock waves for an arbitrary equation of state. *Tech. Rep.* PB-32189. Clearinghouse for Federal Scientific and Technical Information, U.S. Dept. of Commerce, Washington DC.
- BOURLIOUX, A. & MAJDA, A. 1992 Theoretical and numerical structure for unstable two-dimensional detonations. *Combust. Flame* **90**, 211–229.
- CHPOUN, A., PASSEREL, D., LI, H. & BEN-DOR, G. 1995 Reconsideration of oblique shock wave reflections in steady flows. Part 1. Experimental investigation. *J. Fluid Mech.* **301**, 19–35.

- COLELLA, P. & HENDERSON, L. F. 1990 The Von Neumann paradox for the diffraction of weak shock waves. *J. Fluid Mech.* **213**, 71–94.
- COURANT, R. & FRIEDRICHS, K. 1948 *Supersonic Flow and Shock Waves*. Interscience.
- FICKETT, W. & DAVIS, W. C. 1979 *Detonation*. University of California Press, Berkeley, CA.
- FOMIN, V. M., HORNUNG, H. G., IVANOV, M. S., KHARIONOV, A. M. & KLEMONKOV, G. P. 1996 The study of transition between regular and Mach reflection of shock waves in different wind tunnels. In *12th Intl Mach Reflection Symp.* (ed. B. Skews). University of the Witwatersrand, Johannesburg, Republic of South Africa.
- FOWLES, G. 1981 Stimulated and spontaneous emission of acoustic waves from shock fronts. *Phys. Fluids* **24**, 220–227.
- FRITZ, J. N. 1996 Overtaking wave interaction, reflected shock or reflected release? In *Shock Compression of Condensed Matter–1995* (ed. S. C. Schmidt & W. C. Tao), pp. 271–274. APS.
- GLIMM, J., KLINGENBERG, C., MCBRYAN, O., PLOHR, B., SHARP, D. & YANIV, S. 1985 Front tracking and two dimensional Riemann problems. *Adv. Appl. Math.* **6**, 259–290.
- GROVE, J. W. & MENIKOFF, R. 1990 Anomalous reflection of a shock wave at a fluid interface. *J. Fluid Mech.* **219**, 313–336.
- HENDERSON, L. F., COLELLA, P. & PUCKETT, E. G. 1991 On the refraction of shock waves at a slow-fast gas interface. *J. Fluid Mech.* **224**, 1–27.
- HENDERSON, L. F., CRUTCHFIELD, W. Y. & VIRGONA, R. J. 1997 The effects of heat conductivity and viscosity of argon on shock waves diffracting over rigid ramps. *J. Fluid Mech.* **331**, 1–36.
- HENDERSON, L. F. & LOZZI, A. 1975 Experiments on transition of Mach reflexion. *J. Fluid Mech.* **68**, 139–155.
- HENDERSON, L. F. & LOZZI, A. 1979 Further experiments on transition to Mach reflection. *J. Fluid Mech.* **94**, 541–559.
- HORNUNG, H. G. 1986 Regular and Mach reflection of shock waves. *Ann. Rev. Fluid Mech.* **18**, 33–58.
- HORNUNG, H. G., OERTEL, H. & SANDEMAN, R. J. 1979 Transition to Mach reflexion shock waves in steady and pseudosteady flow with and without relaxation. *J. Fluid Mech.* **90**, 541–560.
- HORNUNG, H. G. & ROBINSON, M. L. 1982 Transition from regular to Mach reflection of shock: part 2, the steady-flow criterion. *J. Fluid Mech.* **123**, 155–164.
- IVANOV, M. S., GIMELSHEIM, S. F. & BEYLICH, A. E. 1995 Hysteresis effect in stationary reflection of shock waves. *Phys. Fluids*, **7**, 685–687.
- IVANOV, M. S., GIMELSHEIN, S. F., MARKELOV, G. N. & BEYLICH, A. E. 1995 Numerical investigation of shock wave reflection problems in steady flows. In *20th Intl Sympos. on Shock Waves*, (ed. B. Sturtevant, J. E. Shepherd & H. G. Hornung), pp. 471–476. Graduate Aeronautical Lab., CIT.
- KONTOROVICH, V. M. 1959 Reflection and refraction of sound by shock waves. *Sov. Phys. Acoustics*, **5**, 320–330. Translation from *Akusticheskii Zl.*
- LANDAU, L. D. & LIFSHITZ, E. M. 1959 *Fluid Mechanics*. Addison-Wesley.
- LIU, T.-P. 1976a Shock waves in the nonisentropic gas flow. *J. Diff. Equat.* **22**, 442–452.
- LIU, T.-P. 1976b The entropy condition and the admissibility of shocks. *J. Math. Anal. Appl.* **53**, 78–88.
- MAJDA, A. & ROSALES, R. 1983 Theory for spontaneous Mach stem formation in reacting shock fronts: I. The basic perturbation analysis. *SIAM J. Appl. Maths* **43**, 1310–1334.
- MENIKOFF, R. & PLOHR, B. J. 1989 The Riemann problem for fluid flow of real materials. *Revs. Mod. Phys.* **61**, 75–130.
- MÖLDER, S. 1971 Reflection of curved shock waves in steady supersonic flow. *CASI Trans.* **4**, 73–80.
- MOND, M. & RUTKEVICH, I. M. 1994 Spontaneous acoustic emission from strong ionizing shocks. *J. Fluid Mech.* **275**, 121–146.
- NEUMANN, J. VON 1945 Refraction, intersection and reflection of shock waves. *Tech. Rep. NAVORD 203-45*, BuOrd. Reprint in Taub (1963, pp. 300–308).
- PANTAZAPOL, D., BELLET, J. C. & SOUSTRE, J. 1972 Sur les conditions d'apparition de l'effet de mach dans la reflexion d'une onde de choc oblique en ecoulement supersonique. *C. R. Acad. Sci. Paris, A* **225**, 275.
- SKEWS, B. 1996 Aspect ratio effects in steady shock wave reflection transition studies. In *Symposium on Shock Waves, Japan'96*.
- SPIVAK, M. 1965 *Calculus on Manifolds*. Benjamin.

- SUZUKI, T., SAKAMURA, Y. & YIN, X.-Z. 1995 Shock wave reflection from a cone with attack angles in a symmetric plane. In *20th Intl Symp. on Shock Waves* (ed. B. Sturtevant, J. E. Shepherd & H. G. Hornung), pp. 417–422. Graduate Aeronautical Lab., CIT.
- TAKAYAMA, K. & SASAKI, M. 1983 Effects of radius of curvature and initial angle on the shock transition over concave and convex walls. *Rep. Inst. High Speed Mech.* **46**, 1–30.
- TAUB, A. H. (ed.) 1963 *John von Neumann collected works*, vol. VI. Macmillan.
- TESHUKOV, V. M. 1986 On the shock polar in a gas with general equation of state. *PMM USSR* **50**, 71–75. Translation from *Prikl. Matem. Mekhan.* **50**(1), 98–103.
- TESHUKOV, V. M. 1989 Stability of regular shock wave reflection. *J. Appl. Mech. Tech. Phys.* **30**, 189–196. Translation from *Zh. Prikl. Mekhan. Tekhn. Fiz.* **30**(2), 26–33.
- VUILLON, J., ZEITOUN, D. & BEN-DOR, G. 1995 Reconsideration of oblique shock wave reflections in steady flows. Part 2. Numerical investigation. *J. Fluid Mech.* **301**, 37–50.
- WALLUS, H. & DEMMIG, F. 1995 Converging shock waves: modeling and analysis of structures. In *20th International Symposium on Shock Waves* (ed. B. Sturtevant, J. E. Shepherd & H. G. Hornung), pp. 661–666. Graduate Aeronautical Lab., CIT.
- YANG, J., SASOH, A. & TAKAYAMA, K. 1996 The reflection of a shock wave over a cone. *Shock Waves* **6**, 267–273.
- ZEL'DOVICH, Y. B. & RAIZER, Y. P. 1967 *Physics of Shock Waves and High-Temperature Hydrodynamic Phenomena*, Vol. II. Academic.